

GENERATION OF Q-SWITCHING AND MODE-LOCKING
PULSES WITH YTTRIUM OXIDE BASED SATURABLE
ABSORBER

NOORSYAMILA FAZYANTI BINTI MUSTAFA

FACULTY OF ENGINEERING
UNIVERSITY OF MALAYA
KUALA LUMPUR

2019

**GENERATION OF Q-SWITCHING AND MODE-
LOCKING PULSES WITH YTTRIUM OXIDE BASED
SATURABLE ABSORBER**

NOORSYAMILA FAZYANTI BINTI MUSTAFA

**RESEARCH REPORT SUBMITTED IN PARTIAL
FULFILMENT OF THE REQUIREMENTS FOR THE
MASTER DEGREE OF TELECOMMUNICATION
ENGINEERING**

**FACULTY OF ENGINEERING
UNIVERSITY OF MALAYA
KUALA LUMPUR**

2019

UNIVERSITY OF MALAYA
ORIGINAL LITERARY WORK DECLARATION

Name of Candidate: NOORSYAMILA FAZYANTI BINTI MUSTAFA

Matric No: KQH17006

Name of Degree: MASTER of TELECOMMUNICATION ENGINEERING

Title of Project Paper/Research Report/Dissertation/Thesis (“this Work”):

Generation of Q-Switching and Mode-Locking Pulses With Yttrium Oxide Based Saturable Absorber.

Field of Study: Fiber Laser, Photonic Engineering

I do solemnly and sincerely declare that:

- (1) I am the sole author/writer of this Work;
- (2) This Work is original;
- (3) Any use of any work in which copyright exists was done by way of fair dealing and for permitted purposes and any excerpt or extract from, or reference to or reproduction of any copyright work has been disclosed expressly and sufficiently and the title of the Work and its authorship have been acknowledged in this Work;
- (4) I do not have any actual knowledge nor do I ought reasonably to know that the making of this work constitutes an infringement of any copyright work;
- (5) I hereby assign all and every rights in the copyright to this Work to the University of Malaya (“UM”), who henceforth shall be owner of the copyright in this Work and that any reproduction or use in any form or by any means whatsoever is prohibited without the written consent of UM having been first had and obtained;
- (6) I am fully aware that if in the course of making this Work I have infringed any copyright whether intentionally or otherwise, I may be subject to legal action or any other action as may be determined by UM.

Candidate’s Signature

Date:

Subscribed and solemnly declared before,

Witness’s Signature

Date:

Name:

Designation:

GENERATION OF Q-SWITCHING AND MODE-LOCKING PULSES WITH YTTRIUM OXIDE BASED SATURABLE ABSORBER

ABSTRACT

The report aims to a new saturable absorber (SA) material based on metal oxide for both Q-switching and mode-locking pulses generations. Yttrium Oxide (Y_2O_3) was successfully proposed and demonstrated for realizing both Q-switched and mode-locked Erbium-doped Fiber Lasers (EDFLs). The film SA was prepared through solution casting technique by embedding the Y_2O_3 powder into a polyvinyl alcohol (PVA) host film. With the SA, the Q-switched laser was demonstrated with the frequency is tunable from 70.22 kHz to 99.2 as the pump power is varied from 52.4 mW to 181.5 mW. The shortest pulse width of 2.97 μ s and the maximum pulses energy of 180 nJ were obtained at the pump power of 181.5 mW. By incorporating the film SA along with 200 m long single mode fibre (SMF) into another EDFL cavity, the mode-locked laser was also realized to operate at 1 MHz repetition rate with 460 ns pulse width at pumping power within 181.5 – 246.0 mW. The highest pulse energy was obtained at 25.2 nJ. These indicators suggest that $Y_2 O_3$ film is a good passive SA that can be used to generate both Q-switched and mode-locked pulsed laser operating at 1.55 μ m region.

Keywords: Q-switching, mode-locking, Yttrium oxide, passive saturable absorber.

**PENJANAAN DENYUT PENSUISAN-Q DAN SELAKAN-MOD DENGAN
MENGUNAKAN YTTRIUM OKSIDA SEBAGAI PENYERAP BOLEH TEPU
KESELAMATAN.**

ABSTRAK

Laporan eksperimen ini menyasarkan kepada bahan penyerap boleh tepu keselamatan berasaskan logam oksida untuk kedua-dua denyut penjanaan pensuisan-q dan selakan-mod. Yttrium oksida (Y_2O_3) telah berjaya mencadangkan and mendemostrasikan untuk merealisasikan kedua-dua suis-q and selakan-mod gentian laser terdop Erbium (EDFLs). Filem SA ini telah disediakan melalui larutan teknik penuangan dengan membenamkan serbuk Y_2O_3 ke dalam alcohol polyvinyl (PVA) hos filem. Dengan SA ini, suis-q laser telah mendemonstrasi dengan frekuensi boleh tala dari 70.22 kHz sehingga 99.2 kHz sebagaimana kuasa pam berubah dari 52.4 mW to 181.5 mW. Modulasi lebar denyut tersingkat untuk 2.97 μ s dan maksimum dengut tenaga untuk 180 nJ telah diperolehi di kuasa pam 182.5 mW. Dengan menggabungkan filem SA bersama dengan 200m panjang gentian mod tunggal (SMF) ke dalam kaviti EDFL, selakan-mod laser juga berfungsi untuk beroperasi pada kadar ulangan 1 MHz dengan 460 ns modulasi lebar denyut pada kuasa pam diantara, 181.5 – 246.0 Mw. Denyut tenaga yang tertinggi diperolehi pada 25.5 nJ. Ini menunjukkan cadangan filem Y_2O_3 adalah SA pasif yang terbaik yang boleh digunakan untuk menghasilkan kedua-dua suis-q and selakan-mod yang beroperasi pada 1.55 μ m region.

Kata kunci: Pensuisan-Q, Selakan-mod, Yttrium Oksida, Pasif penyerap boleh tepu keselamatan

ACKNOWLEDGEMENTS

I am very appreciated to my supervisor, Prof. Ir. Dr. Sulaiman Wadi Harun. He gave me very in-time valuable instructions and put me in contact with Nur Farhanah and Farina Saffa , who gave me extensive guidance regarding experimental issues.

Furthermore, I also would like to express my sincere gratitude to my family members who has always believed in me on completing this project with flying colors.

In a nut shell, not forgotten, a big thank you to every individual who has provided me the spirit to complete this report.

Universiti Malaya

TABLE OF CONTENTS

GENERATION OF Q-SWITCHING AND MODE-LOCKING PULSES WITH YTTRIUM OXIDE BASED SATURABLE ABSORBER ABSTRACT	iii
PENJANAAN DENYUT PENSUISAN-Q DAN SELAKAN-MOD DENGAN MENGGUNAKAN YTTRIUM OKSIDA SEBAGAI PENYERAP BOLEH TEPU KESELAMATAN ABSTRAK.....	iv
Acknowledgements	v
Table of Contents	vi
List of Figures	viii
List of Tables.....	x
List of Symbols and Abbreviations.....	xi
CHAPTER 1: INTRODUCTION.....	1
1.1 Problem Statement and Research Motivation.....	1
1.2 Objectives	3
1.3 Outline of this report.....	4
CHAPTER 2: LITERATURE REVIEW.....	5
2.1 Erbium-doped Fiber Laser.....	5
2.2 Saturable Absorber	7
2.3 Q-switching.....	9
2.4 Mode-locking.....	12
CHAPTER 3: Q-SWITCHED ERBIUM DOPED FIBER LASER WITH YTTRIUM OXIDE BASED SATURABLE ABSORBER	18
3.1 Introduction.....	18

3.2	Preparation and Characterization of Y_2O_3 SA.....	20
3.3	Laser Configuration.....	23
3.4	Results and Discussion.....	24
 CHAPTER 4: MODE-LOCKED FIBER LASER WITH YTTRIUM OXIDE BASED SATURABLE ABSORBER.....		31
4.1	Introduction.....	31
4.2	Nonlinear characteristic of the Y_2O_3 film based SA.....	32
4.3	Mode-locked laser cavity configuration.....	33
4.4	Result and Discussion.....	35
 CHAPTER 5: CONCLUSION.....		40
	References.....	42

LIST OF FIGURES

Figure 2.1: Energy level diagram for Erbium ion. Dashed and solid lines indicate the fast phonon and radiative transition, respectively.....	7
Figure 2.2: Pulse shaping mechanism by a SA.....	8
Figure 2.3: Resonant cavity modes and the gain spectrum of a laser for (a) single mode lasing (b) multimode lasing.....	13
Figure 2.4: The output pulse train in time domain when (a) No phase coherence between the multiple longitudinal modes (b) 10% of the modes are phase coherence (c) all the modes are phase coherence.....	14
Figure 2.5: Mode-locked pulses in (a) the time and (b) frequency domain (Keller, 2003)	17
Figure 3.1: Illustration of the fabrication process for the Y_2O_3 thin film	20
Figure 3.2: Y_2O_3 PVA thin film characteristics (a) physical image (b) SEM image (c) EDS profile (d) linear absorption profile	22
Figure 3.3: Experimental setup of the proposed Q-switched EDFL using Y_2O_3 PVA film SA. Inset shows the fabricated Y_2O_3 PVA attached onto the fiber ferrule.....	24
Figure 3.4: Output spectrum of Q-switched EDFL at the threshold pump power of 52.4 mW.....	25
Figure 3.5: Oscilloscope pulse train at pump power of (a) 52.4 mW (b) 123.4 mW (c) 181.5 mW.....	27
Figure 3.6: RF spectrum at pump power of 123.4 mW	28
Figure 3.7: Repetition rate and pulse width of Q-Switched EDFL.....	29
Figure 3.8: Output power and pulse energy of Q-switched EDFL	30
Figure 4.1: (a) The balanced twin-detector measurement system for measuring nonlinear absorption of Y_2O_3 film. (b) The measured saturable absorption characteristic of the film	33
Figure 4.2: Configuration of Y_2O_3 film-based mode-locked EDFL.....	35
Figure 4.3: Important characteristics of the Y_2O_3 based mode-locked EDFL at 181.5 mW pump power (a) Output spectrum (b) Oscilloscope trace (c) A single pulse envelop (d) RF spectrum, while the inset shows the fundamental frequency in detail.	38

Figure 4.4: The output power and pulse energy of the mode-locked EDFL as a function of pump power (181.5-246.0 mW).39

Universiti Malaya

LIST OF TABLES

Table 2.1: Common laser-active ions, host glasses and lasing wavelength for various rare-earth doped fibers.....	5
--	---

Universiti Malaya

LIST OF SYMBOLS AND ABBREVIATIONS

Al_2O_3	:	Aluminium Oxide
Bi_2Se_3	:	Bismuth Selenide
Bi_2Te_3	:	Bismuth Telluride
CW	:	Continuous-Wave
EDF	:	Erbium-Doped Fiber
EDFA	:	Erbium-Doped Fiber Amplifier
EDFL	:	Erbium-Doped Fiber Laser
Er^{3+}	:	Erbium
FESEM	:	Field Emission Scanning Electron Microscopy
FSF	:	Frequency Shifting Feedback
FWHM	:	Full Width Half Maximum
Ho^{3+}	:	Holmium ion
ISO	:	Isolator
MOPA	:	Master Oscillator Power Amplifier
MoS_2	:	Molybdenum Disulfide
MoSe_2	:	Molybdenum Diselenide
Nd^{3+}	:	Neodymium
NiO	:	Nickel Oxide
NPR	:	Nonlinear Polarization Rotation
OSA	:	Optical Spectrum Analyzer
Pr^{3+}	:	Praseodymium
PLD	:	Pulsed Laser Deposition
PVA	:	Polyvinyl Alcohol

RF	:	Radio Frequency
SA	:	Saturable Absorber
SESAM	:	Semiconductor Saturable Absorber Mirrors
SHB	:	Spatial Hole Burning
SNR	:	Signal to Noise Ratio
TiO ₂	:	Titanium Dioxide
TI	:	Topology Insulators
Tm ³⁺	:	Thulium
TMDS	:	Transition-Metal Dichalcogenides
WDM	:	Wavelength Division Multiplexing
WS ₂	:	Tungsten Disulfide
Yb ³⁺	:	Ytterbium
ZnO	:	Zinc Oxide

CHAPTER 1: INTRODUCTION

1.1 Problem Statement and Research Motivation

The technological progress in laser technology of today was preceded by a long history of research and development. It started as early as 1960s when the rare-earth-doped fiber laser was demonstrated. Fiber lasers use rare-earth-doped fiber as a gain medium. They are more compact due to fibers can be easily bent and coiled compared to gas and solid-state lasers. There are also many benefits of fiber laser such as high power, high stability and high reliability that average life span almost to 100,000 hours and very efficient. This fiber doped with ions of a rare-earth element such as Erbium (Er^{3+}) ions that operate at a wavelength of around $1.5 \mu\text{m}$. These ions are doped in the core glass matrix, resulting in high absorption with low loss in the visible and near-infrared spectral regions. Normally, doped fiber laser is integrated into the fiber laser oscillator to generate a broad spectrum with a relatively high gain. Erbium-doped fiber lasers (EDFLs) are widely researched in the recent years due to their many advantages such as simplest way of doping, compact, high output power, high reliability and very cost effective. This type of laser uses Er^{3+} ions in an Erbium-doped fiber (EDF) to generate laser at 1550 nm region with 980 nm or 1480 nm pumping through a process of stimulated emission.

Pulsed EDFLs have become an attracted device for a wide range of multi-purpose applications, such as remote sensing, telecommunications, engineering, material processing and medicine. They are more compact with high resolution and fast processing due to high repetition rate as compared to the radio waves and microwaves. These lasers can be constructed by using two approaches; Q-switching or mode-Locking techniques. Q-switched lasers are generally used to generate high pulse energy

at relatively low repetition rate (kHz) and a pulse with much longer pulse duration. Mode-locked lasers on the other hand generates a laser with high repetition rate (MHz) and narrow pulse width.

Q-switched and mode-locked fiber laser can be produced by either active or passive techniques. Passive technique has the most advantages in term of compactness, flexibility and simplicity in design as compared to the active technique. In the active technique, it uses an external element such as acousto-optic or electro-optic modulator to induce pulse. This modulator, it requires complex circuit to control it and thus the cost will be increased and effort to create the pulse laser system. Thus, passive technique was introduced by the invention of saturable absorber in order to solve the problem facing in active technique.

Saturable absorbers (SA) are substances that reduce the absorption of light by increasing the light intensity. It is used in a laser cavity to generate pulses. To date, many SAs have been developed such as semiconductor saturable absorber mirrors (SESAMs) (Vasseur, 2006) and Single-Wall Carbon Nanotubes (SWCNTs) (M. E. Fermann & Hartl, 2013). Nevertheless, the function of the SAs are subjected to be limited because of many factors such as limited operating bandwidth, complex optical alignments, environmental sensitivity and also due to the complexity of the fabrication process. Recently, graphene has become one of the most massive and promising materials as a SA (Skorczakowski et al., 2010). Graphene and SWCNTs are obtained from carbon and have excellent optical characteristics such as ultra-fast recovery times and also high saturable absorption rates. Both materials are significantly easier and cheaper to fabricate as compared to SESAM. Therefore, it stands for crucial advantage. SWCNTs also have good optical characteristics as a SA due to the operational

wavelength is chosen by the diameters of the individual nanotubes. This has then leads to about a boundary in its operating wavelength and power tuning.

Transition metal oxides-based as SA such as Zinc Oxide (ZnO) nanoparticles, Titanium Dioxide (TiO₂) nanoparticles and Iron Oxide (Fe₂O₃) are also explored for laser applications. In this research work, passive Q-switched and mode-locked EDFLs are proposed and demonstrated using new metal oxide material based on Ytterium oxide (Al₂O₃) as SA. The SA is integrated in the EDFL cavity by sandwiched the prepared SA film in between two fiber ferrules to achieve a stable pulse train with a well repetition rate, pulse width and peak power. The performance of both lasers is compared and discuss in this report.

1.2 Objectives

The research work aims to demonstrate Q-switched and mode-locked EDFL using a newly developed metal oxide saturable absorbers (SA) based on Yttrium oxide (Y₂O₃). This research embarks on the following objectives:

1. To fabricate and characterize Y₂O₃ SA
2. To demonstrate and evaluate the generation of Q-switched pulse train using the developed SA
3. To demonstrate and evaluate the generation of mode-locked pulse train using the developed SA

1.3 Outline of this report

This report describes an experimental work on both Q-switched and mode-locked EDFL using a new type of SA based on metal oxide material. The content is arranged in five chapters including the introduction and conclusion chapter. Chapter 1 explained the problem statement, motivation and objectives of this research work. In Chapter 2, literature reviews on optical fiber, laser, saturable absorber and pulses generation through Q-switching and mode-locking processes are documented. Chapter 3 demonstrates the fabrication of Y_2O_3 based SA and the demonstration of Q-switched EDFL using the fabricated film SA. The Y_2O_3 film was prepared by embedding the Y_2O_3 into PVA film based on drop and dry process. The film is sandwiched between two fiber ferrule connectors with a fiber adapter to form a fiber-compatible SA. Chapter 4 demonstrates a mode-locked nanosecond EDFL utilizing Y_2O_3 based SA. Finally, Chapter 5 concludes the finding of the research work and proposes some recommendations for future work.

CHAPTER 2: LITERATURE REVIEW

2.1 Erbium-doped Fiber Laser

The invention of rare-earth doped fiber has spurred the rapid progress on optical fiber laser technology especially on Q-switching and mode-locking pulses generations. Typically, fiber lasers use a glass fiber which the core was doped with rare-earth ions as a gain medium. The rare-earth fiber is then pumped with a laser diode to provide an external energy to excite the active ions onto the excited state and create the population inversion in the gain medium. The rare earth ions can absorb light in which it stimulates them into the meta-stable levels to allow the light amplification via the stimulated emission. This behavior is very helpful for creating laser, long lifetimes of the metastable states, quantum efficiency also inclined to be high or to amplify the signal at the emission wavelength. The example of the rare earth ions that are using in fiber doped gain medium such as Erbium (Er^{3+}), Thulium (Tm^{3+}), Ytterbium (Yb^{3+}), Holmium (Ho^{3+}), Neodymium (Nd^{3+}) and Praseodymium (Pr^{3+}). Table 2.1 shows the rare earth ions and its host glasses and also their emission wavelength ranges.

Table 2.1: Active ions, host glasses and lasing wavelength for various rare-earth doped fibers

Active ions	Common host glasses	Emission wavelength (μm)
Neodymium (Nd^{3+})	Silicate and Phosphate glasses	1.0 – 1.1 μm
Ytterbium (Yb^{3+})	Silicate glass	1.0 – 1.1 μm
Erbium (Er^{3+})	Silicate, Phosphate and Fluoride glasses	1.55 – 1.62 μm , 2.7- 3.0 μm
Thulium (Tm^{3+})	Silicate, Germanate and Fluoride glasses	1.7 – 2.1 μm
Praseodymium (Pr^{3+})	Silicate and Fluoride glasses	1.3 μm
Holmium (Ho^{3+})	Silicate and fluorozirconate glasses	2.1, 2.9 μm

Since the invention of the Erbium-doped fiber (EDF) in late 1980s, it has been used in broad range of applications as an optical amplifiers and fiber lasers. Erbium-doped fiber lasers (EDFLs) have been extensively studied and investigated for use in communication system that operates in the 3rd communication window ranging from 1520nm to 1565nm. They can generate continuous wave and pulses laser outputs operating in broad wavelength range based on the $^4\text{I}_{11/2} \rightarrow ^4\text{I}_{15/2}$ transition in Erbium ions. Figure 2.1.1 illustrates the energy level of Erbium ions (Er^{3+}) in silica fibers. The Erbium ions (Er^{3+}) can be excited by either 980 nm or 1480 nm pump. For example, with 980 nm pumping, the ions are excited to the upper level before they undergo a rapid, non-radiative decay to long-lived metastable state, $^4\text{I}_{13/2}$. These ions can stay for relatively long periods of time (8~10ms) at this state. The quantum level efficiency of a medium is depending on how long it can stay in the metastable state. More photons are required to be excited if they relax too quickly to the lower level. That means more input pump power is needed to make the amplifier work. The same mechanism can be

used to explain the working principle of EDFA too. Active ions from the metastable state will eventually fall to the lower level (ground state) $^4I_{15/2}$ resulting either spontaneous emission as it goes through along the fiber. This Erbium ions (Er^{3+}) also can be excited to the upper level by 1480 nm pumping as shown in Figure 2.1 but this is typically undesirable. When pump at 1480 nm, it creates interactions that decreases the efficiency of the active medium and also increases the amplifier noise. This happens because pumping process and stimulated emission are occurring in the same wavelength and energy band. In close cavity setup, the Amplified Spontaneous Emission (ASE) will oscillate and produce laser through the stimulated emission process.

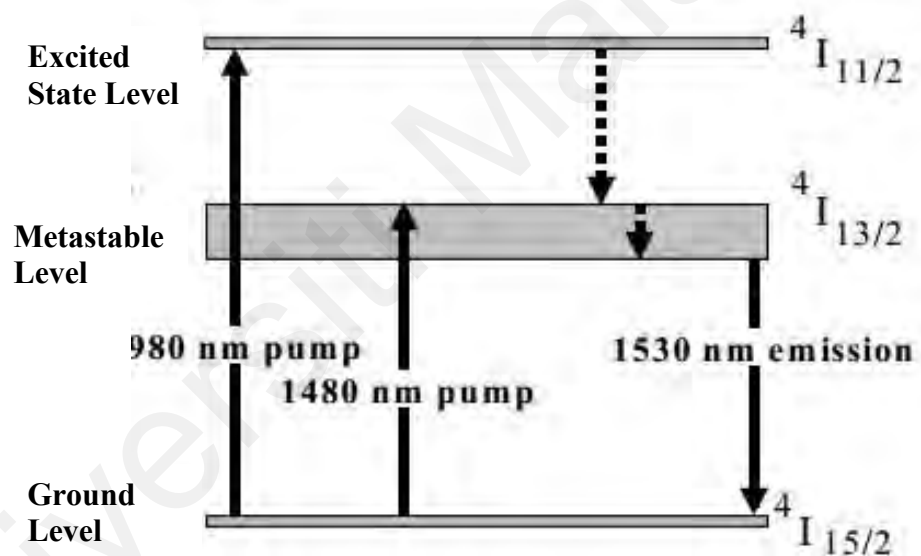


Figure 2.1: Energy level diagram for Erbium ion. Dashed and solid lines indicate the fast phonon and radiative transition, respectively.

2.2 Saturable Absorber

A saturable absorber (SA) is an optical component with a certain optical loss that is reduced at high optical intensities. SA can be widely divided into two categories that are real SAs and artificial SAs. Real SAs are materials that exhibit an intrinsic nonlinear decrease in absorption with the increasing light intensity. Artificial SAs in

contrast, are devices that exploit nonlinear effects to duplicate the action of the real SA by inducing an intensity-dependent transmission. In this section, we will only concentrate on the real SAs to explore the advantages of it such as engineerable properties, switching speed and broadband operation. An ideal SA have high damage threshold but it is time and cost efficient. The primary applications of SA are used in Q-Switching and Passive Mode-Locking of lasers such as generation of short optical pulses. SA also is helpful for the purposes of nonlinear filtering outside laser resonators such as for cleaning up pulse shapes and in optical signal processing.

Figure 2.2 shows the change of pulse shape when passing through a SA. The low-intensity leading and trailing parts of each pulse are attenuated more strongly than its high-intensity pulse center as shown in the figure. This makes the newly formed pulses getting shorter and shorter over several iterations until a pulse-width of just a few femtoseconds is attained. The width of this pulse then depends on the gain bandwidth of the gain material and on the response time of the SA. The more frequencies that the gain material produces in a laser, such as the more modes generated inside the laser cavity, the narrower the pulse become. In the same way, as a general trend, the faster a SA can respond to the light, the shorter the pulse become.

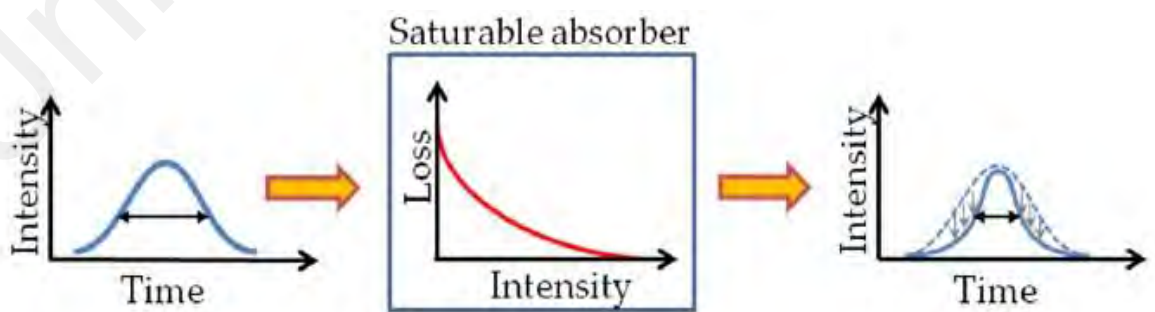


Figure 2.2: Pulse shaping mechanism by a SA.

2.3 Q-switching

Q-switching is also known as a giant pulse formation or Q-spoiling, is a technique to generate a pulse laser. In general, Q-switching laser is a pulsed laser with the ability to store maximum potential energy and generate huge energetic pulses within a short time domain (typically in the range of nanoseconds) by modulating its intra-cavity losses mechanism. The Q value (also known as the quality factor) can be calculated by the equation (Xinju, 2010) :

$$Q = 2\pi\nu_o \left(\frac{\text{energy stored in cavity}}{\text{energy lost per second}} \right) \quad (2.1)$$

where ν_o represents the laser's central frequency. To further simplify the equation, the assumption made is as follow:

- W represents energy stored within the cavity.
- δ denotes the rate of energy loss for single-path light propagation within the laser cavity.

Suppose L represents the resonator length, n represents the medium's refractive index, and c represents light velocity, then the duration of single-path light propagation in a laser cavity is given as:

$$\tau = \frac{c}{nL} \quad (2.2)$$

If the energy loss per second is given by;

$$\delta = \frac{\delta Wc}{nL}$$

and equation (2.1) becomes

$$Q = 2\pi\nu_o \frac{W}{\delta Wc/nL}$$

$$= \frac{2\pi nL}{\delta\lambda_o} \quad (2.3)$$

where λ_o is the central wave length of laser in the vacuum.

Q value is inversely proportional to the resonator loss (δ) with the condition values of λ_o and L are definite (equation 2.3) and their relationships with the light oscillation occurring within the laser's cavity are as summarized below:

- a) When Q value is low due to high loss (δ), the oscillation initiation threshold is increased, making initiation harder.
- b) When Q value is high due to minimal loss (δ), oscillation is easily started due to the resulting low initiation threshold.

Based on equation 2.3, laser's threshold can be easily modified by applying a sudden change to the loss (δ) or the Q value of the resonator (Xinju, 2010). Changes in δ of a resonator will modify the Q value accordingly, resulting in a Q-switched operation. The modulation of δ within the laser's cavity can be performed either actively or passively, using modulators or SAs respectively. The mechanism underlying the Q-switch operation involves the building up of a large inversion by the pumping of laser while the resonator losses are sustained at high levels, resulting in a large gain of stored potential energy in the laser medium. When the resonator δ is reduced abruptly, the stored energy is then released in the form of an intense pulse (Gupta & Ballato, 2006). Usually, spontaneous emission denotes the start of pulse growth. The high initial inversion will drop and peaks again, producing pulses. Generally, Q-switched lasers are applied in fields that need short pulses but with high pulse energies and peak powers (Siegman, 1986).

Active Q switching involves the use of external means to modulate the loss inside the laser cavity, such as the use of an acousto-optic modulator (AOM) – diffract and change light frequency using sound waves (Riesbeck & Lux, 2009) or electro-optic modulator (EOM) – modify phase, frequency, amplitude or polarization of light beam using an optical device with electro-optic effect (Foster et al., 2006; Zhao et al., 2000), thereby controlling the output characteristics of the generated pulse.

In contrast to its active counterpart, a passively Q-switched laser does not require an external modulator as the cavity loss is controlled by SA. This makes passive Q-switching low cost, easier to implement and simpler to operate (D. Popa et al., 2011; Popa et al., 2010).

There are several types of SAs with different parameters, for different applications, including metal doped crystals (Laroche et al., 2002; Philippov, Kir'yanov, & Unger, 2004), Semiconductor saturable absorber mirrors (SESAMs) (U. Keller, 2003; Spuhler et al., 2005), SWCNTs (F. Ahmad et al., 2014; Ismail et al., 2012; Rozhin, Sakakibara, Tokumoto, Kataura, & Achiba, 2004), graphene (Ferrari et al., 2006; Haris et al., 2015; Yang et al., 2014), graphene oxide (GO) (Adnan et al., 2016a; Markom et al., 2018; Saleh et al., 2014) and reduced graphene oxide (rGO) (Guo et al., 2012; S. Liu et al., 2012; Yin et al., 2012). There are also devices that exhibit decreasing optical losses for higher densities artificially by polarization effect, such as the nonlinear polarization rotation (NPR) (Anyi, Haris, Harun, Ali, & Arof, 2013; Matniyaz, 2018; W. Wang et al., 2012). The transmission of SA is dependent on the incoming light intensity, i.e., absorption will occur to light with low intensity while light with high intensity will be released, based on the recovery period.

2.4 Mode-locking

The term mode-locking refers to the requirement of phase locking many different frequency modes of a laser cavity. This locking has the result of inducing a laser to produce a continuous train of extremely short pulses rather than a CW of light. In principle, though, a continuous train of pulses can be generated by a Q-switching technique as described in the previous sub-section. The difference between these two pulsing mechanism lies in the optical phase of the pulses. The mode locked pulses are phase coherent with each other, while the Q switched pulses are not. This simple fact has massive implications in regards to the application of these two types of lasers.

To understand the mode locking process, we will begin by looking at a CW laser with a Fabry-Perot cavity in the frequency domain. Figure 2.3 (a) shows a single longitudinal mode CW laser where only one resonant mode of the laser cavity ($\nu=c/2nL$) overlaps in frequency with the gain medium. Thus, the laser emits a CW beam with a narrow range of frequencies ($E(t) = E_1 e^{i(\omega_1 t + \phi_1)}$). In general, however, the gain medium could overlap with several modes and the output of such a laser can be described in the time domain as:

$$E(t) = \sum_n^N E_n e^{i(\omega_n t + \phi_n)} \quad (2.4)$$

where the sum is over all of the lasing cavity modes, E_n is the amplitude of the n^{th} mode, ω_n is the angular frequency of the n^{th} mode, and ϕ_n is the phase of the n^{th} mode. For the single-mode laser, this sum just has one term as given above. As we will see, the phase term plays the key role in the difference between incoherent multimode lasing and mode locking.

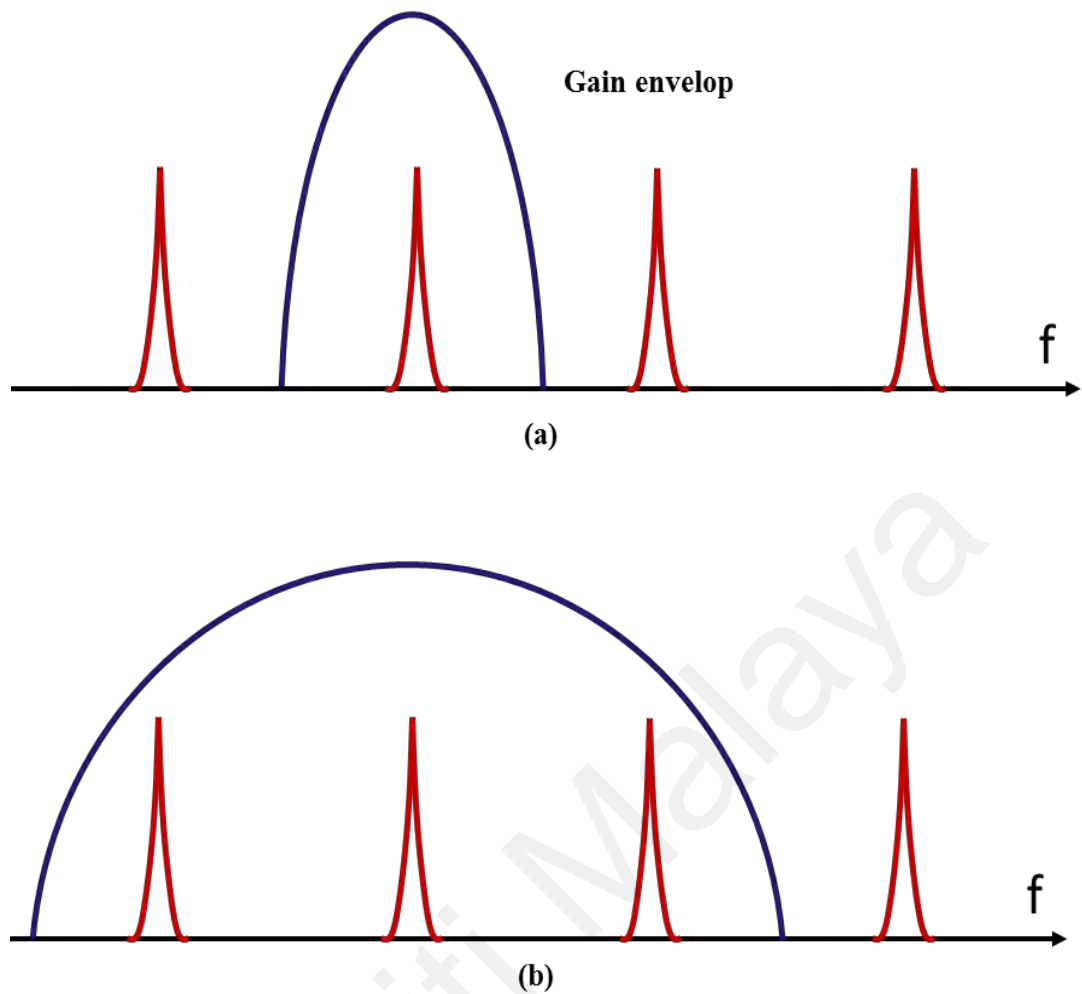


Figure 2.3: Resonant cavity modes and the gain spectrum of a laser for (a) single mode lasing (b) multimode lasing

As the gain bandwidth of the laser is increased to overlap with more of the cavity modes as shown in (Figure 2.3 (b)), multimode lasing will be generated. In this configuration, there are 3 terms in Equation (2.4). The output of such a laser depends critically on the phase relationship between the 3 modes. If each mode has a randomly varying phase with respect to the other modes, then a time domain detector on the output would show us that the laser is emitting a CW beam with a large amount of intensity noise as shown in (Figure 2.4 (a)), while a frequency domain detector would show us that the energy was contained in narrow spikes (with lots of intensity noise) spaced evenly by the free spectral range (FSR) of the cavity. However, if we can fix the relative phases to a set value, then the situation changes dramatically (Figure 2.4(b) and

(c)). With fixed phase relationships, the three modes can combine to interfere in such a way as to constructively interfere at multiples of the roundtrip time of the cavity, while they destructively interfere elsewhere. This process creates shorter pulses as the number of phase locked modes increases.

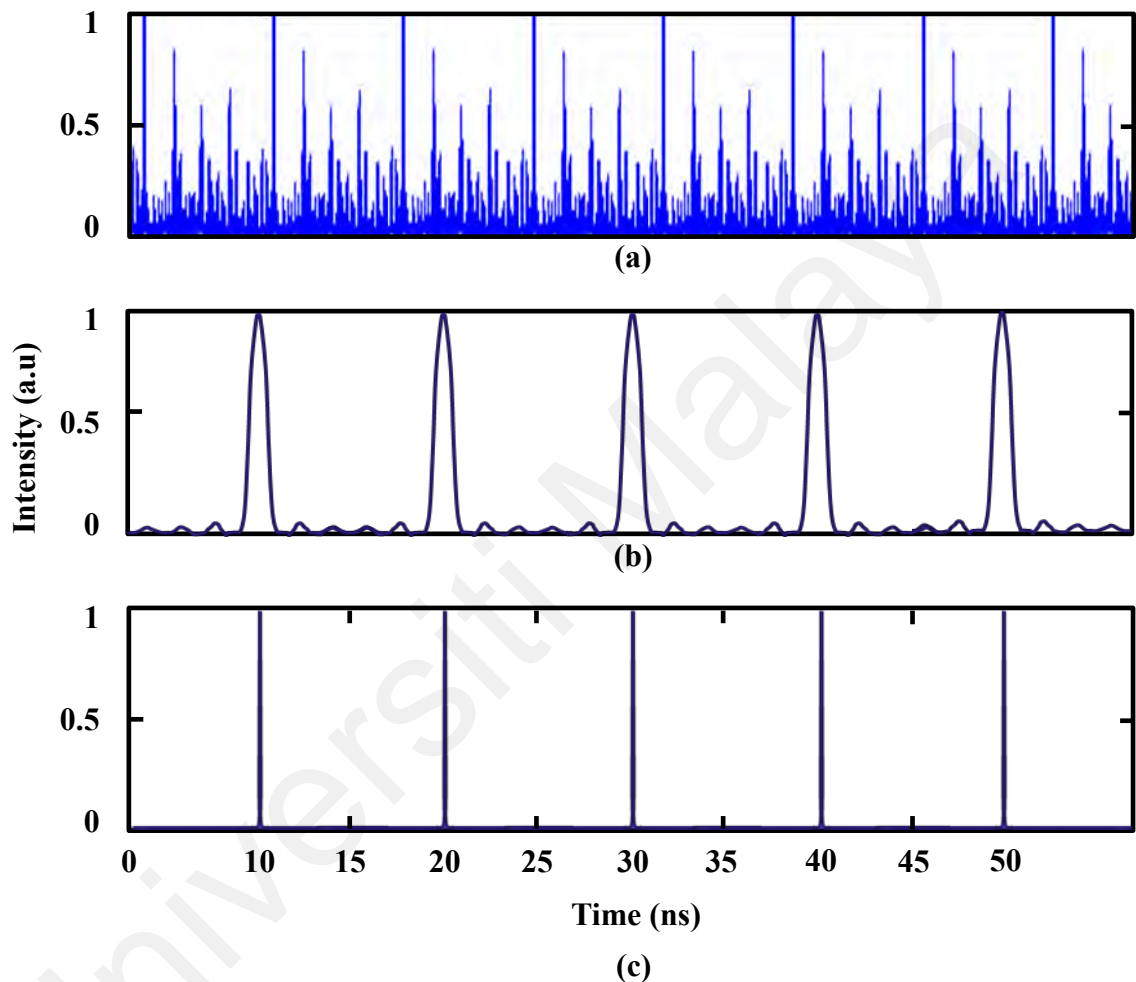


Figure 2.4: The output pulse train in time domain when (a) No phase coherence between the multiple longitudinal modes (b) 10% of the modes are phase coherence (c) all the modes are phase coherence.

Mode-locking is a technique to generate an ultrashort pulse laser. It can be realized using a passive technique based on SA. An ultrashort pulse can emerge when a SA modulates the loss once per cavity round-trip and all longitudinal modes have a fixed phase relationship (Faubert & Chin, 1982; Meiser, 2013; Trebino, 2012). Thus,

the mode-locking of the oscillating laser produces an ultrashort pulses train (ranging from ns to fs duration) at defined repetition rate in MHz corresponding to the free spectra range of laser cavity or the number of obtained pulses per second (M. Fermann, Galvanauskas, Sucha, & Harter, 1997; Haus, 2000; Riidiger Paschotta & Keller, 2003). The estimation of pulse repetition rate, f in passive mode-locking technique is given by;

$$\text{Repetition rate, } f \text{ (ring cavity)} = \frac{c}{nL} \quad (2.5)$$

where c , n , and L denote the speed of light ($3 \times 10^8 \text{ms}^{-1}$) refractive index of the medium (1.46 for silica fiber), and total cavity length, respectively. It is shown from the equation that the repetition rate is determined by the total cavity length for a passive mode-locking, and therefore, the higher pulse repetition rate is obtained for a shorter cavity length.

The pulse width of the laser indicates the full width at half maximum (FWHM) of the power versus time and a very short pulse width can be realized by a mode-locked laser. The higher numbers of longitudinal modes that have a fixed phase relationship can translate to a shorter pulse width. The short pulse duration of the mode-locking mode is useful for many applications including fast optical data transmission, and time-resolving process. The relationship between pulse width and bandwidth of the optical fiber pulses is referred to a time bandwidth product (TBP). As described by the principle of Heisenberg, the TBP of the pulse is impossible to drop below a limit of TBL,

$$T_{BL} \leq \Delta t \times \Delta v \quad (2.6)$$

where Δt and Δv denotes the temporal width (in seconds) and the spectral width (in hertz) of the pulse, which measured at FWHM. The limit of TBP or T_{BL} is depended on

the pulse shape. The bandwidth of the pulse is depended on the spectral bandwidth and operating wavelength of the output spectrum of the laser. It is given as;

$$\text{The bandwidth (BW)} = \Delta\lambda \times \frac{c}{\lambda^2} \quad (2.7)$$

where $\Delta\lambda$ is th spectral bandwidth at FWHM, and λ is the center of the wavelength of output spectrum. The pulse width is given as;

$$\text{Pulse width (PW)} = \frac{T_{BL}}{BW} \quad (2.8)$$

From both equations (2.7) and (2.8), it is obtained that the pulse width can also be estimated from a given optical bandwidth. Generally, the pulse width of mode-locking pulses is usually measured by using an auto-correlator, which its function according to the estimated pulse shape. The pulse shape consists of Gaussian, and Secant hyperbolic, depending on the output spectrum, characteristic of the mode-locking operation, and total cavity dispersion. The Gaussian pulse shape is obtained when the cavity dispersion is closed to zero or equal to zero as in a stretched pulse laser. Mode locking methods can be divided into two classes: active and passive. In active mode locking, some external source is used to drive the mode locking element, while in passive mode locking a saturable absorber is commonly used.

Mode locked pulses in time and frequency domains are shown in (Figure 2.5). In the time domain, the mode locked laser produces an equidistant pulse train, with a period defined by the round-trip time of a pulse inside the laser cavity T_R and a pulse duration τ_p (U. Keller, 2003). In the frequency domain, this results in a phase locked frequency comb with a constant mode spacing that is equal to the pulse repetition rate $\nu_R = 1/T_R$. The spectral width of the envelope of this frequency comb is inversely

proportional to the pulse duration. The fundamental repetition rate of a mode lock laser is determined by its cavity length, as shown in the equations below.

$$\text{Repetition rate (for linear cavity)} = \frac{c}{2nL} \quad (2.9)$$

$$T_R = \frac{2nL \text{ (for linear cavity) or } nL \text{ (for ring cavity)}}{c} \quad (2.10)$$

Equations (2.9) and (2.10) can be used to calculate the fundamental repetition rate for linear and ring cavity respectively. Here, c , n and L represents the speed of light, refractive index and length of the cavity respectively. As the round-trip time, T_R , is the inverse of repetition rate, therefore, T_R is depending on the cavity type. Sometimes the repetition rate can be some integer multiple of the fundamental repetition rate. In this case, it is called harmonic mode locking (Becker et al., 1972).

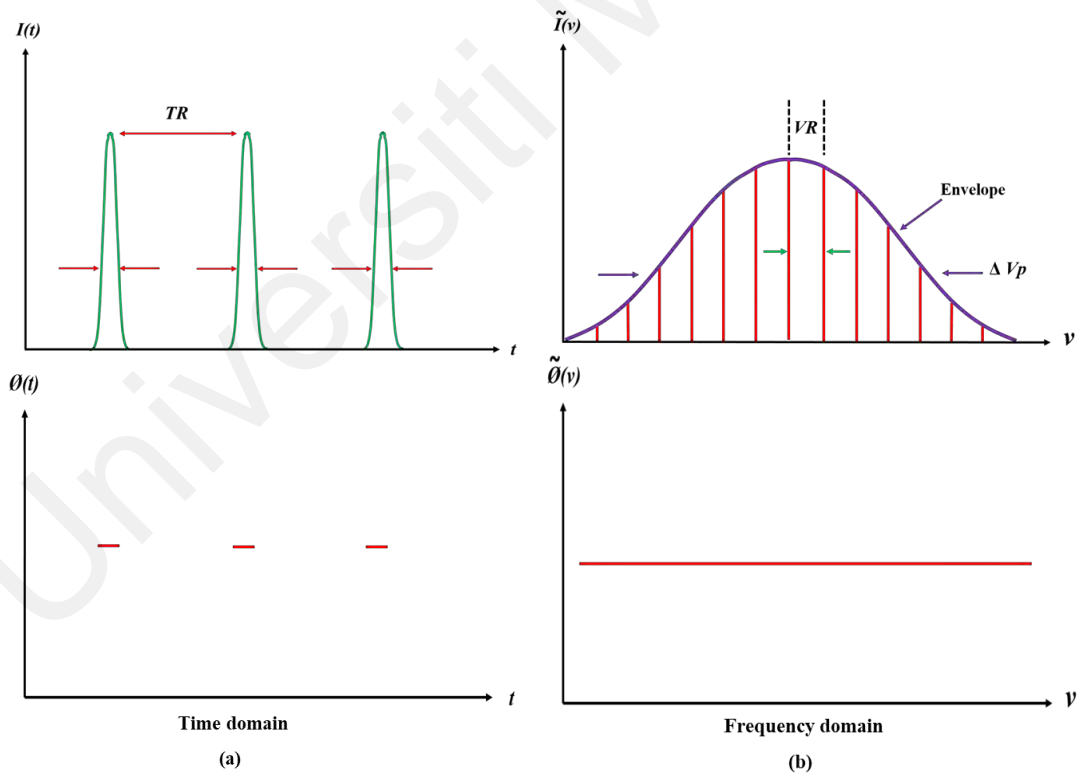


Figure 2.5: Mode-locked pulses in (a) the time and (b) frequency domain (Keller, 2003)

CHAPTER 3: Q-SWITCHED ERBIUM DOPED FIBER LASER WITH YTTRIUM OXIDE BASED SATURABLE ABSORBER

3.1 Introduction

Q-switched fiber lasers have drawn tremendous interests in recent years due to their many potential applications in telecommunication, medical diagnostics and treatments, sensing, material processing, and range finding (Hakulinen & Okhotnikov, 2007; Lucas & Zhang, 2012; R Paschotta et al., 1999). They can be generated by either active or passive methods. The active method normally uses an external acousto-optic modulator to modulate the intra-cavity light and generate pulsed laser in the cavity (Svelto & Hanna, 1998). On the other hand, the passive method employs the saturable absorption of optical material to change the intra-cavity light. Compared with the active method, the passive Q-switching based on saturable absorbers (SAs) has significant advantages of compactness, simplicity and flexibility of implementation (Z.-C. Luo, Liu, Wang, Luo, & Xu, 2012).

Passive Q-switched fiber lasers can be realized by many techniques such as employing nonlinear polarization rotation (NPR) scheme to modulate the intra-cavity light (Z.-C. Luo et al., 2012). Semiconductor saturable absorbers (SESAMs) (Keller et al., 1992; M. Wang, Chen, Huang, & Chen, 2014), carbon nanotubes (CNTs) (Set, Yaguchi, Tanaka, & Jablonski, 2004; Zhou, Wei, Dong, & Liu, 2010), graphene (Bao et al., 2011; Liu, Xu, & Wang, 2012; Z. Luo et al., 2010; Daniel Popa et al., 2011) and black phosphorus (BP) (Y. Chen et al., 2015) have also been successfully used as intracavity-loss modulators to produce pulsed lasers passively. After its debut in 1992 (Keller et al., 1992), SESAMs quickly became the most prominent SA for several years. However, they suffer from some drawbacks including narrow absorption bandwidth,

relatively high production cost and considerably bulky size. The main drawback of CNT SAs is that their absorption efficiency and bandwidth are dependent on their diameter. As for graphene, its main issue is its relatively low optical absorption per layer that limits its usability. Meanwhile, BP is a polarization dependent and hydrophilic material that easily interacts with water (Island, Steele, van der Zant, & Castellanos-Gomez, 2015). Thus, constructing a BP SA is challenging as it requires a complex preparation as well as careful handling. In recent years, other new materials that are relatively easy to prepare have been proposed as candidates for SAs to produce cheap and stable pulsed fiber lasers (Ab Rahman et al., 2018; Kang et al., 2018; Li et al., 2015; Niu, Chen, Sun, Man, & Zhang, 2017). For instance, Rahman et al. used holmium oxide based SA to produce stable Q-switched fiber laser at the 2-micron regime (Rahman et al., 2017).

Yttrium oxide (Y_2O_3) or yttria, is an air-stable, white solid substance, which is normally used as a common starting material for inorganic compounds. It has proven to be a useful coating material for high power UV lasers (ref). In combination with silicon dioxide it produces an effective dual wavelength antireflection coating at 351 and 1054 nanometers which has good resistance to damage at both wavelengths. Optically, it has been shown to have enough linear absorption at 1.5 μm region, suggesting that it is suitable to be used for producing Q-switched laser operating in that region. By properly embedding sufficient Y_2O_3 element into the polyvinyl alcohol (PVA), a very thin Y_2O_3 PVA film with a thickness of around 30 μm could be formed. Then a small piece (1 mm x 1 mm) of the film is placed between two fiber ferrules to construct a fiber compatible SA. The SA can be used to realize a simple and flexible all fiber passively-Q-switched laser system.

In this chapter, a stable passively Q-switched EDFL employing a Y_2O_3 SA in a ring cavity is reported. We believe that this is the first time that an all fiber Q-switched laser employing such a SA is reported. The laser operates at 1560.5 nm wavelength with

an initial repetition rate of 70.22 kHz at the threshold pump power of 52.4 mW. The repetition rate of the pulses increases as the input power is increased. At the maximum available pump power of 181.5 mW, the repetition rate of the pulsed laser is 99.2 kHz.

3.2 Preparation and Characterization of Y_2O_3 SA

The Y_2O_3 film was fabricated by mixing Y_2O_3 powder and polyvinyl alcohol (PVA) solution as described in Figure 3.1. At first, we prepared the PVA solution by mixing 1 g of PVA powder with 120 ml deionized water as a solvent. To totally dissolve the solute PVA, this mixture was stirred at 90 °C, and then it was cooled down to room temperature. 10 mg of Y_2O_3 powder was then mixed into 10ml of the prepared PVA solution. The Y_2O_3 PVA solution was further stirred for at least an hour with a magnetic stirrer. The mixed solution was then sonicated for about three hours in ultrasonic bath. This process completely dispersed the powder by breaking the bond between the molecules that were bound by the Van der Waals force. Finally, the homogenous solution obtained was dispensed onto a small glass Petri dish. It is allowed to dry for approximately 48 hours at room temperature to form a thin film with a thickness of about 50 μm

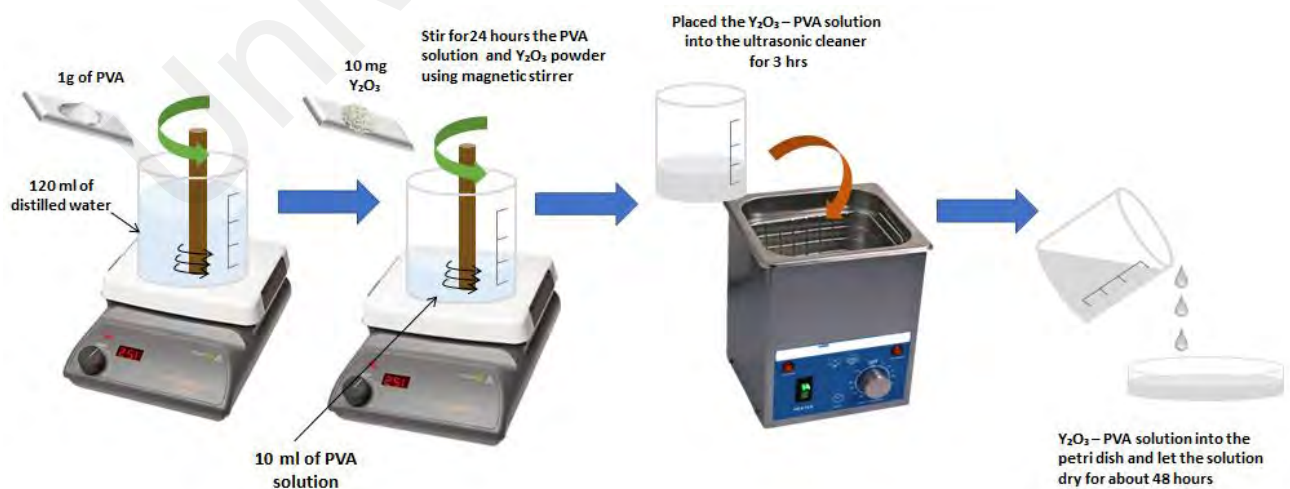
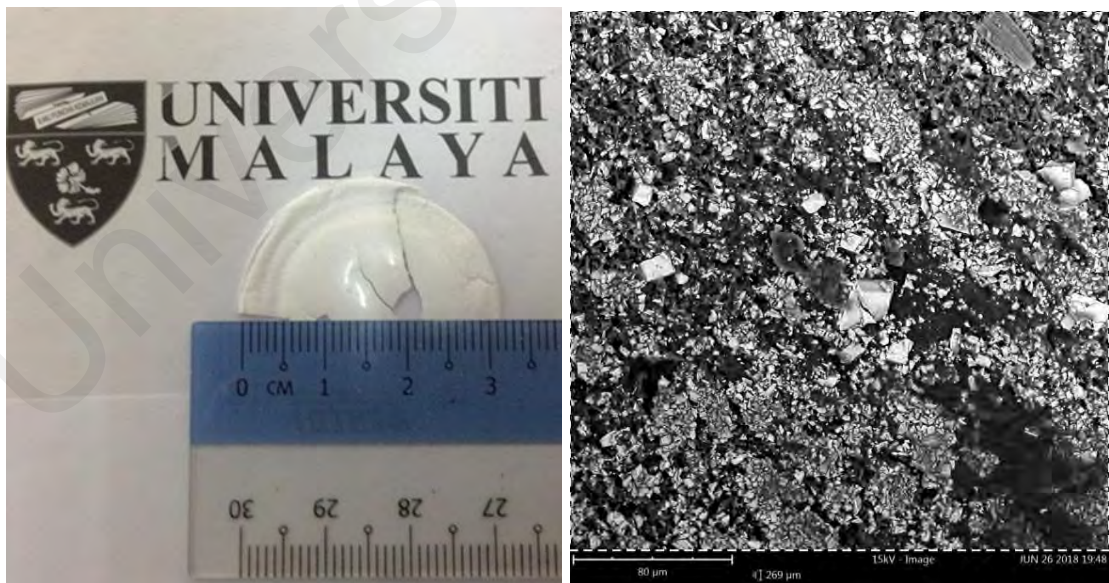


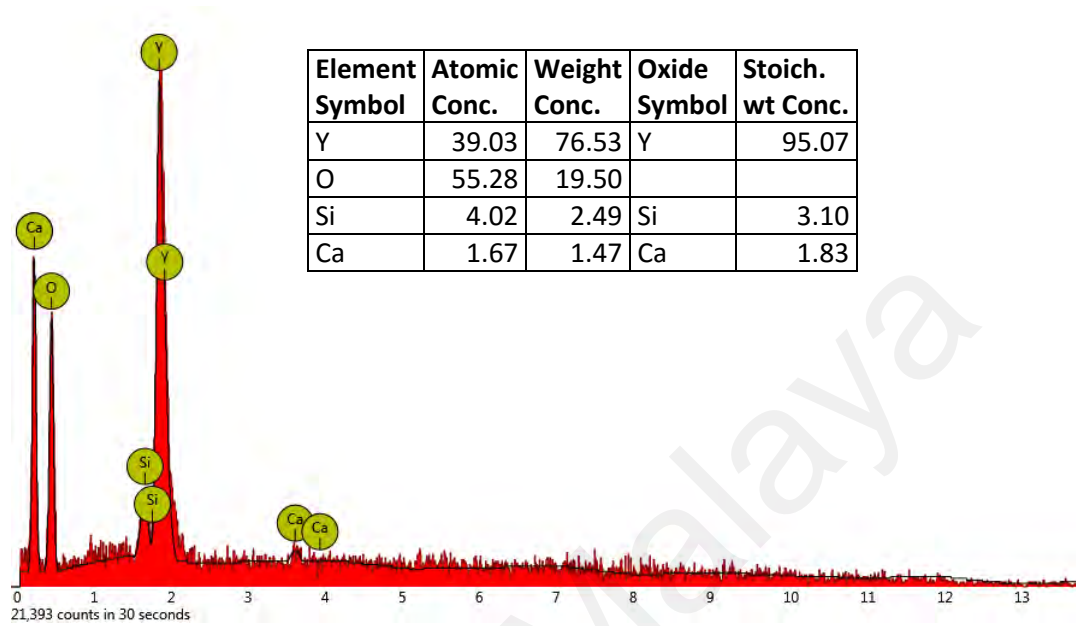
Figure 3.1: Illustration of the fabrication process for the Y_2O_3 thin film

Figure 3.2(a) shows the real image of the Y_2O_3 PVA thin film. The white thin film is partly transparent and the SA base-material (Y_2O_3) seems to be distributed evenly across the film as vindicated by the scanning electron microscope (SEM) image in Figure 1(b) which shows an almost consistent topography. The Energy dispersive X-ray spectroscopy (EDS) in Figure 1(c) affirms the presence of Yttrium and Oxygen elements in the film. The initial indicator of a SA is its optical absorption. Figure 1(d) shows the linear optical absorption profile of the Y_2O_3 PVA film which shows that the SA optically absorbs around 9.2 dB at the Q-switched laser operating wavelength of 1560 nm. The SA was made by sandwiching a tiny piece of the thin film (about 1 mm x 1 mm) between two clean FC/PC fiber ferrules. Prior to that, a small quantity of index matching gel was applied on the fiber ferrule surface, to easily stick the film SA onto the ferrule tip as well as to minimize the unwanted parasitic reflections between the coupling areas. The use of Y_2O_3 PVA film as SA is demonstrated in the following fiber laser experiment.

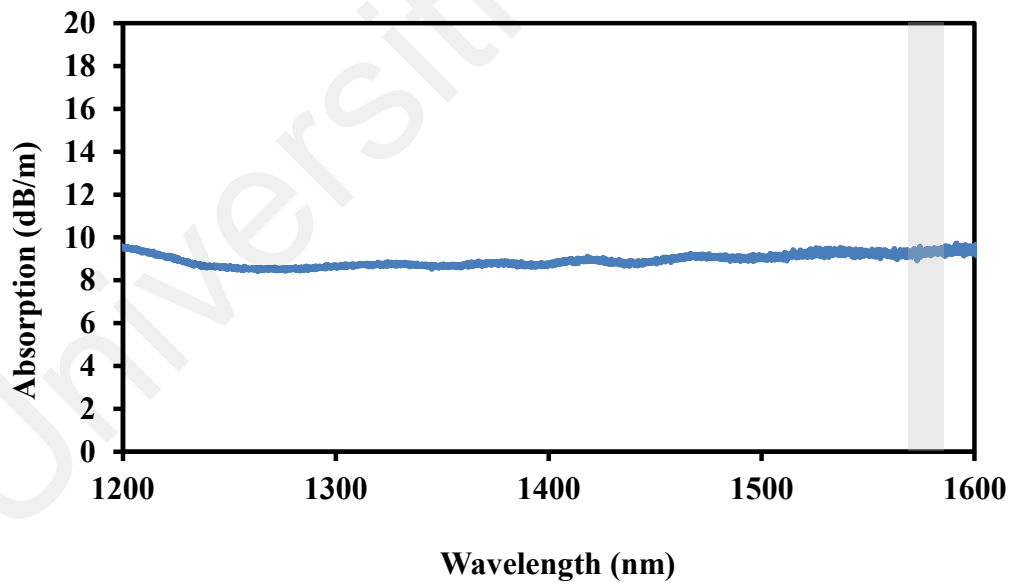


(a)

(b)



(c)



(d)

Figure 3.2: Y_2O_3 PVA thin film characteristics (a) physical image (b) SEM image (c) EDS profile (d) linear absorption profile

3.3 Laser Configuration

Figure 3.3 shows the schematic diagram of the proposed Q-switched EDFL, which based on forward-pumped ring cavity scheme. The fabricated Y_2O_3 PVA was sandwiched in between two fiber connectors via a fiber adapter to form a fiber-compatible SA device, which is then integrated into the laser cavity for the Q-switching operation. Inset of Figure 3.3 shows the fabricated Y_2O_3 PVA attached onto the fiber ferrule. The laser cavity consists of 2.4 m long erbium-doped fiber (EDF) gain medium, a wavelength division multiplexer (WDM), an isolator, SA device and a 80/20 output coupler. The components are all connected via standard SMF. The EDF has a core diameter of 4 μm , a fiber diameter of 125 μm , an absorption coefficient in the range of 23 dB/m at an operating wavelength of 980 nm and a numerical aperture (NA) of 0.23. It is pumped by a 980 nm single wavelength laser diode (LD) via the 980 nm port of the 980/1550 nm wavelength division multiplexer (WDM). The other end of the gain medium is connected to the optical isolator which ensures unidirectional light propagation inside the cavity. Then the light goes into the thin-film SA that periodically switches the intracavity losses, as well as, the Q-factor of the cavity. After the SA, the light passes through the 80/20 output coupler where 20% of the laser output is extracted while the rest (80%) is retained to circulate inside the cavity via the 1550 nm port of the WDM. An optical spectrum analyzer (OSA) with a 0.07 nm resolution is utilized to investigate the laser optical spectrum. Meanwhile, a radio frequency spectrum analyzer (RFSA) and a digital oscilloscope (OSC) that are pre-coupled with a fast photodetector (PD) are used to examine the appearance and quality of the pulsed signal in the time domain and frequency domain, respectively. An optical power meter is used to measure the output power of the pulsed laser.

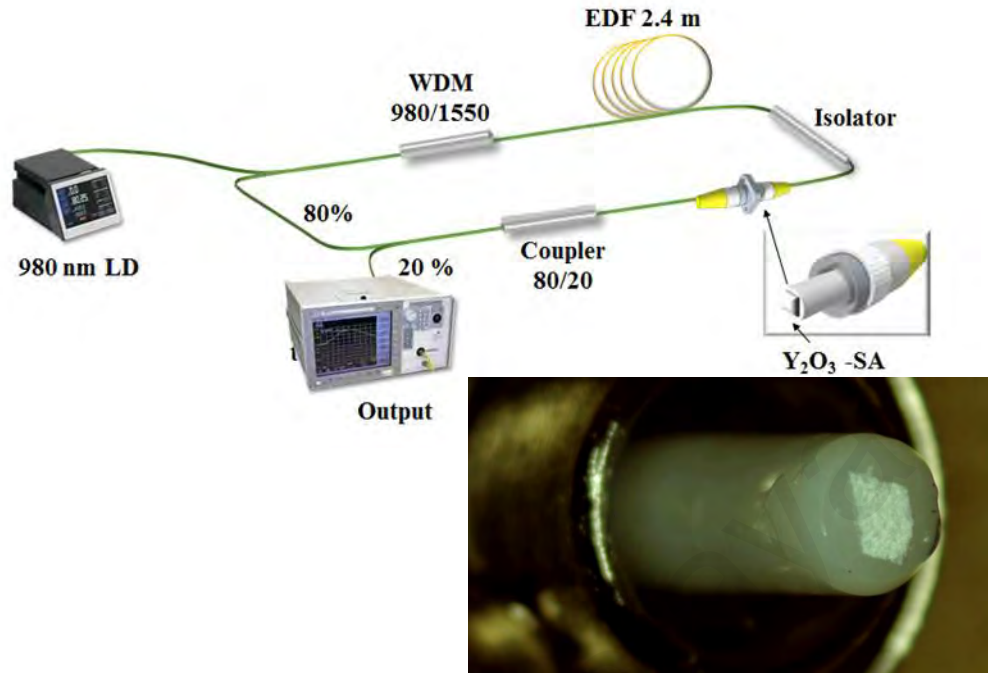


Figure 3.3: Experimental setup of the proposed Q-switched EDFL using Y₂O₃ PVA film SA. Inset shows the fabricated Y₂O₃ PVA attached onto the fiber ferrule.

3.4 Results and Discussion

Without the SA, the EDFA generated a continuous wave (CW) laser operating at 1565 nm as the pump power was increased above the threshold pump power of about 30 mW. With a SA inside the cavity, the proposed laser started to transform into a stable Q-switched laser with an initial frequency of 70.22 kHz at a threshold pump power of 52.4 mW. The pulsed laser remains stable with the increase in pump power and its frequency rose steadily up to 99.2 kHz when the pump power reached the maximum power of 181.5 mW. Figure 3.4 shows the optical spectrum of the laser, which is centered at 1560.5 nm with a bandwidth of 0.5 nm. It is observed that the operating wavelength is shifted to shorter wavelength with the incorporation of SA device in the cavity. This is attributed to the increased cavity loss that forces the operating

wavelength to shift to higher gain region to compensate for the loss. To confirm that the Q-switched pulses were attributed to the Y_2O_3 , the Y_2O_3 film was removed from the laser cavity. In this case, we observed that no pulses on the oscilloscope even when the pump power was adjusted over a wide range. This finding has verified that the Y_2O_3 film was responsible for the Q-switching operation of the EDFL. The optical signal-to-noise ratio (OSNR) of the spectrum is obtained at 45 dB, which is acceptable.

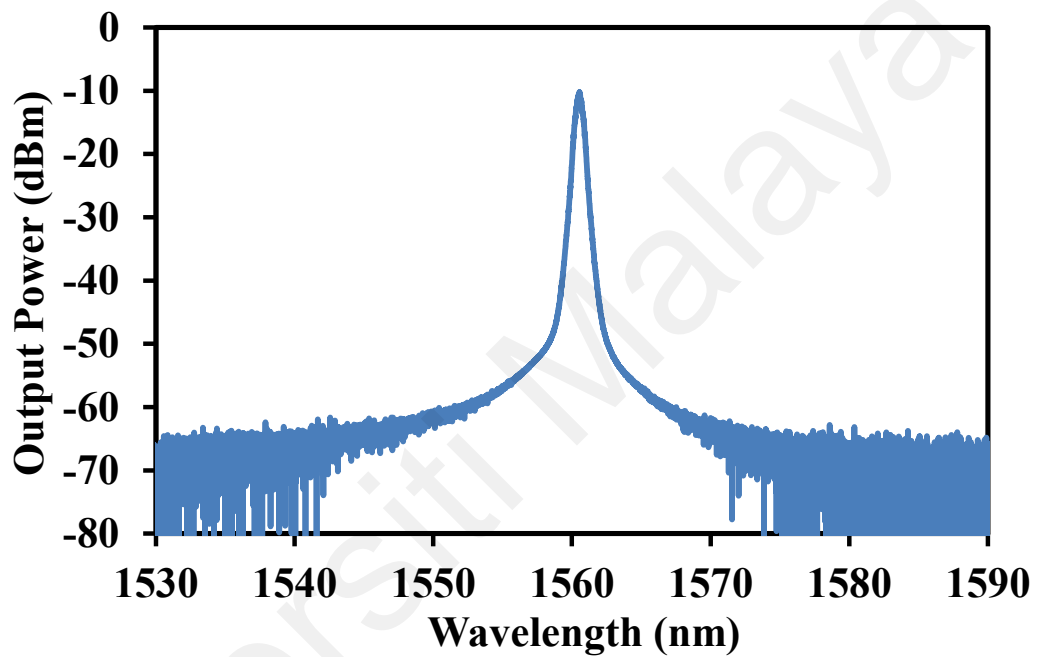
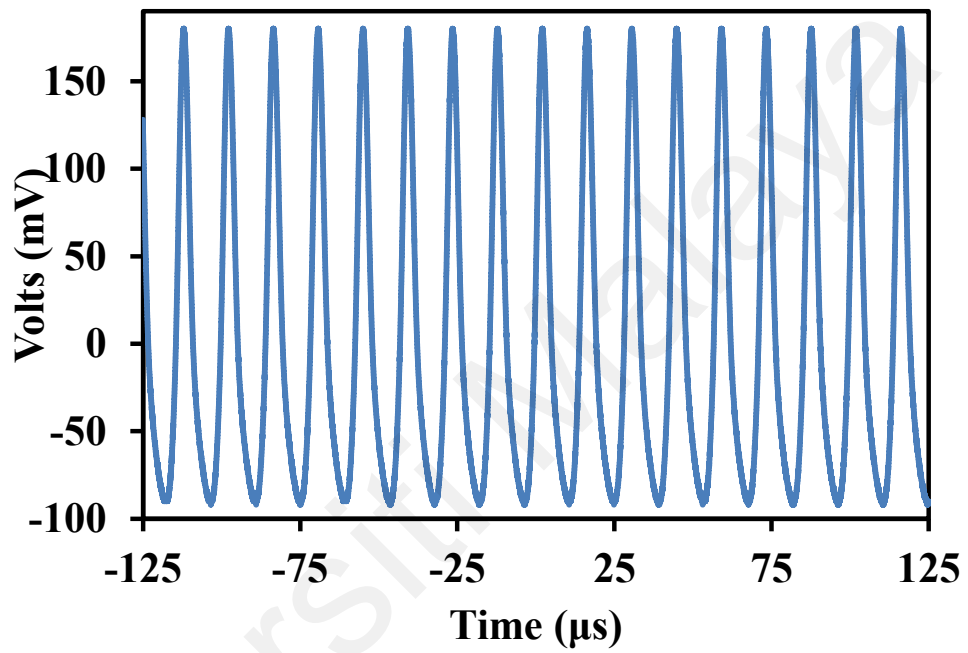


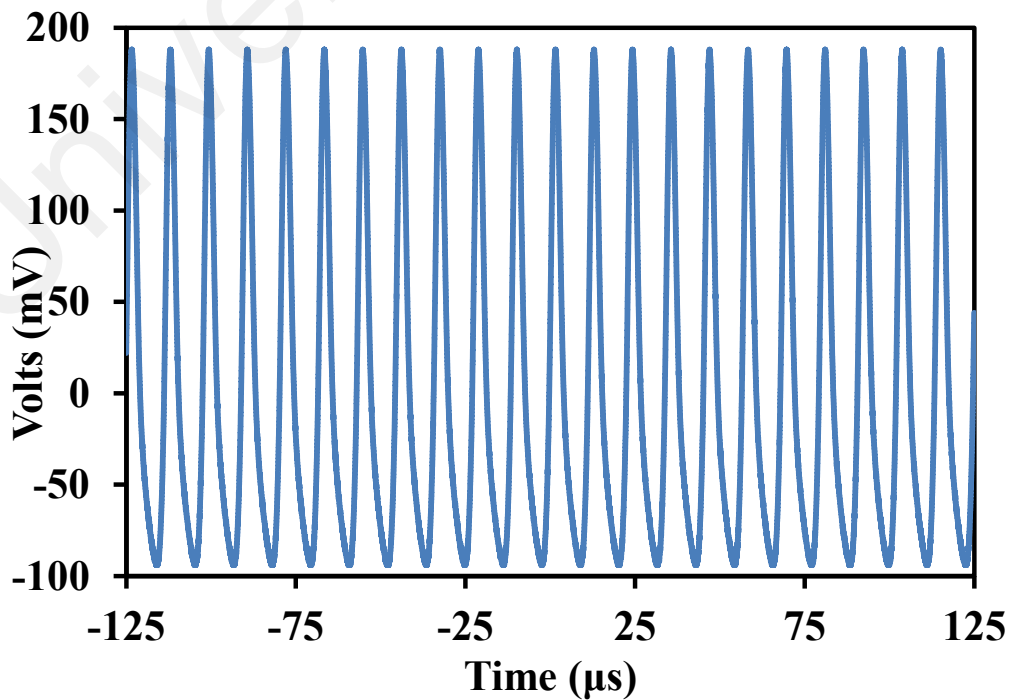
Figure 3.4: Output spectrum of Q-switched EDFL at the threshold pump power of 52.4 mW

Figures 3.5(a), (b) and (c) show the Q-switched pulse trains at three different pump powers of 52.4, 123.4 and 181.5 mW respectively. As the pump power increases, more energy can be stored in the laser cavity and these attributes to the rise in the repetition rate accompanied by the reduction in pulse duration. The pulse periods (peak to peak time intervals) were measured to be 14.24, 11.36 and 10.08 μ s, which corresponded to the repetition rates of 70.22, 88.03 and 99.22 kHz, at pump power of 52.4, 123.4 and 181.5 mW, respectively. These typical Q-switching pulse train were

stable with no significant pulse jitter seen on the oscilloscope. The single pulse envelopes for these pulses train display a symmetrical Gaussian-like shape and the full-width half-maximum (FWHM) were measured to be 4.2, 3.3 and 3.0 μs at pump power of 52.4, 123.4 and 181.5 mW, respectively. The properties of the Q-switching laser principally rely on upon the gain medium, SA and pump power.



(a)



(b)

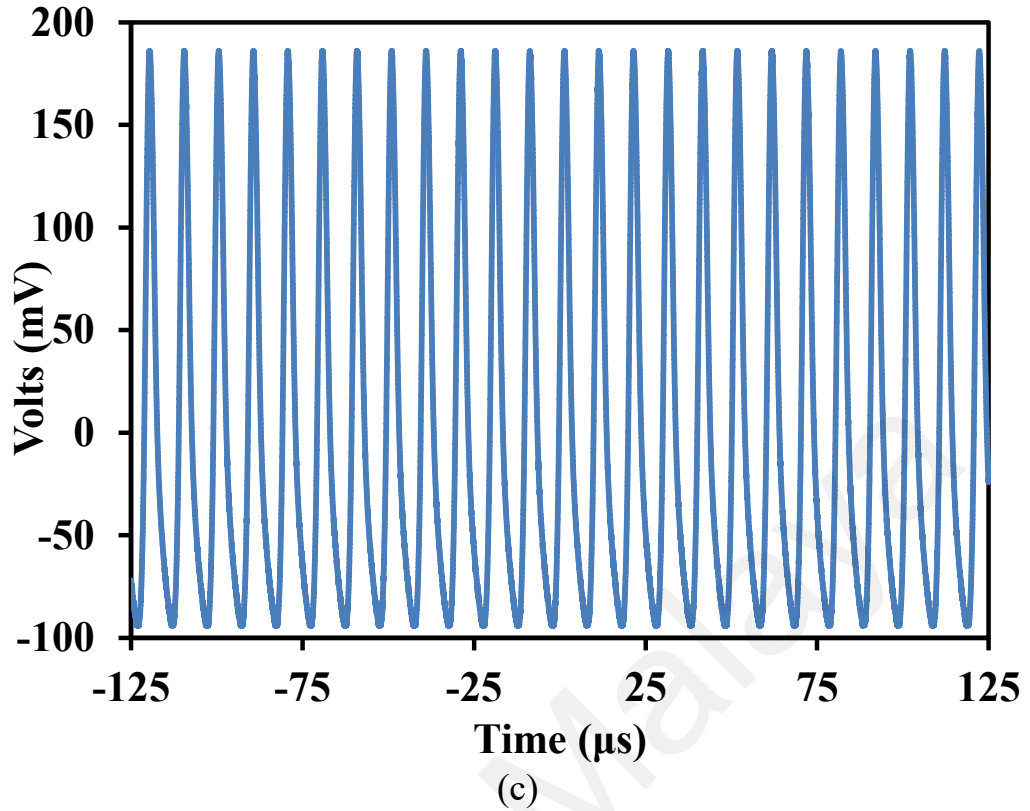


Figure 3.5: Oscilloscope pulse train at pump power of (a) 52.4 mW (b) 123.4 mW (c) 181.5 mW.

Meanwhile, the frequency domain of the EDFL was also examined via the RFSA to evaluate the stability of the Q-switching operation as depicted in Figure 3.6. In the measurement, the pump power was fixed at 123.4 mW. The RF spectrum obtained shows that more than ten frequency harmonics generated stably within the span of 1300 kHz. As expected, the fundamental frequency was obtained at 88.03 kHz, which is in good agreement with the time domain of Figure 3.5(b), thus technically confirming both optical measurements. The signal-to-noise ratio (SNR) was ~ 58 dB with no spectral modulation, indicating excellent Q-switching stability.

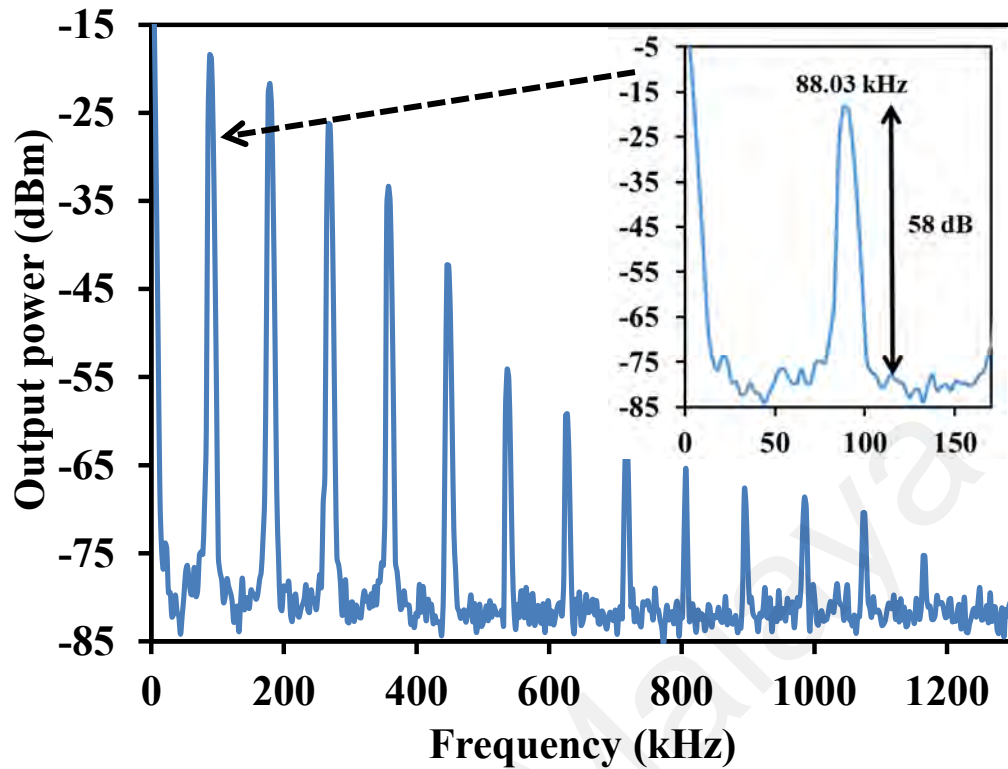


Figure 3.6: RF spectrum at pump power of 123.4 mW

In order to further investigate the performances of the Q-switched laser, the output pulses characteristics such as the repetition rate, pulse duration, output power, and pulse energy were studied with respect to the incident pump power. Figure 3.6 shows the pulse repetition rate and pulse width of the laser as functions of the incident pump power. As illustrated in the figure, the repetition rate increases nearly monotonously from 70.2 to 99.2 kHz, while the pulse width decreased from 4.21 μ s to 2.97 μ s as the pump power is boosted from 52.4 mW to 181.5 mW. These are typical features of passive Q-Switching pulse train. By increasing the pump power, more gain was provided to saturated the SA. Hence, the threshold energy stored in the EDF to generate a pulse was reached earlier. As a result, the repetition rate is increasing while the pulse width is reducing. The Q-switched pulse output was stable with no significant pulse-intensity fluctuation on the oscilloscope as the pump power was increased.

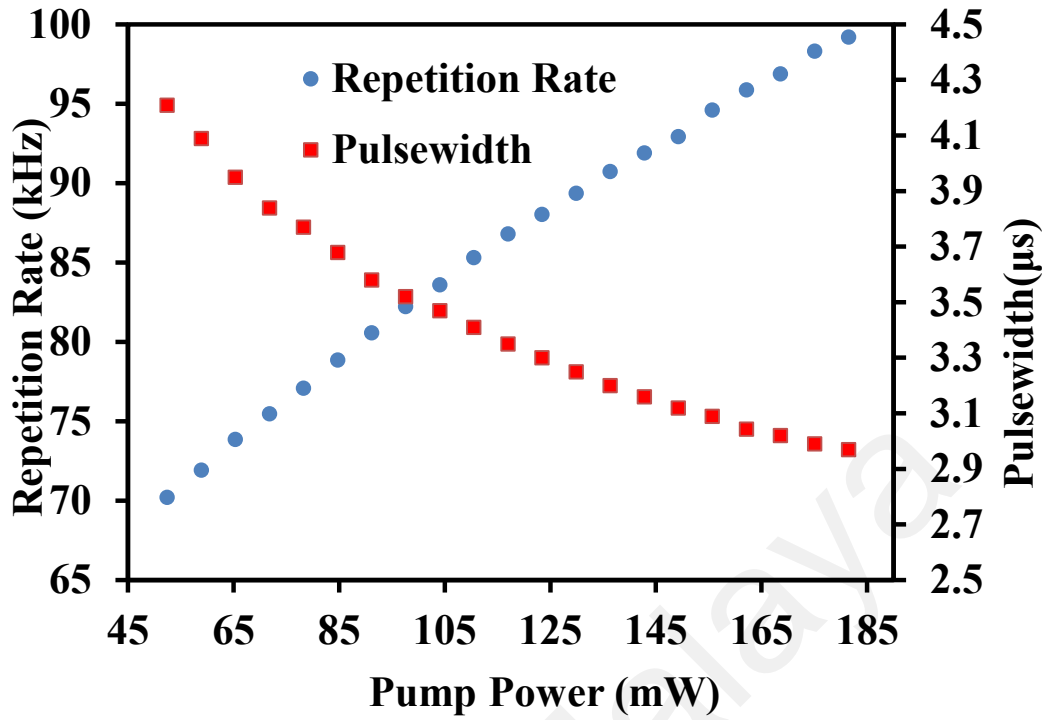


Figure 3.7: Repetition rate and pulse width of Q-Switched EDFL

Figure 3.8 shows the output power of the pulse and correspondingly calculated the single pulse energy against the pump power. The output power increases linearly from 7.93 mW to 17.86 mW as the pump power increases from 52.4 mW to 181.5 mW. This is equally to 7.71 % slope efficiency. The pulse energy also increases linearly with the pump power. The maximum pulse energy was 180 nJ. These results demonstrate that the Y_2O_3 has good potential as SA for Q-switched fiber lasers operating at 1.5-micron region.

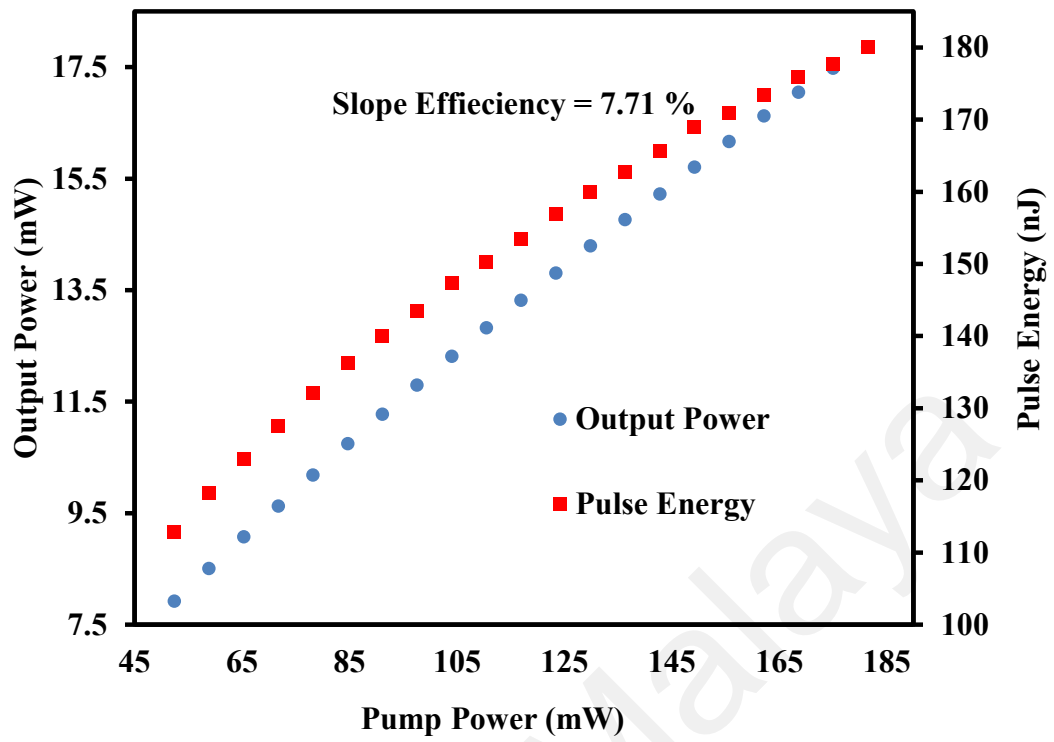


Figure 3.8: Output power and pulse energy of Q-switched EDFL

CHAPTER 4: MODE-LOCKED FIBER LASER WITH YTTRIUM OXIDE BASED SATURABLE ABSORBER

4.1 Introduction

Mode-locked fibre lasers typically based on passive technique, have received tremendous responses in recent years owing to their great flexibility and improved simplicity. Unlike the active technique which uses electronically pulse triggering system for the pulse generation, the passive one, is generally much simpler in preparation, smaller in geometry, cheaper, and even faster (Ab Rahman et al., 2018). Mode-locked erbium-doped fibre lasers (EDFL) have found significant potentials in several applications including telecommunication, medical diagnostics and treatments, sensing, material processing, and range finding (Adnan et al., 2016b; F Ahmad et al., 2014). On the other hand, metal oxide nanoparticles have drawn attention due to their stable optical, electrical and structural properties (Noda, Muramoto, & Kim, 2003). For instance, several works have been reported on the nonlinear optical properties of Al_2O_3 , which are suitable to induce pulse generation (Lin, Yang, Liou, Yu, & Lin, 2013).

In this chapter, we report for the first time, to the best of our knowledge, a passively stable and compact mode-locked EDFL by integrating Y_2O_3 PVA composite thin film in the ring cavity to function as saturable absorber (SA). A stable mode-locked EDFL operating at 1560.9 nm with a corresponding pulse repetition rate of 1 MHz and a pulse width of 460 ns were achieved at a pump power range of 181.5-246.0 mW. The SA film is capable to generate mode-locking pulses that has many fields of applications such as in sensing, spectroscopy and as a laser source for second harmonic generation on top of being easy to prepare and cost effective.

4.2 Nonlinear characteristic of the Y₂O₃ film based SA

We designed a balanced twin-detector measurement system to investigate the nonlinear optical absorption characteristics of the fabricated Y₂O₃ film. The measurement system is shown in Figure 4.1(a), which consists of an amplified picosecond fiber laser, a variable optical attenuator (VOA), a 3-dB optical coupler and two power-meters. The laser source is a home-made pico-second Erbium doped fiber laser (repetition rate: 1 MHz, pulse width: 3 ps and central wavelength: 1560 nm). The laser was amplified by a commercial EDFA for obtaining high peak power to sufficiently saturate the Y₂O₃ film. By gradually changing the input power, a series of optical transmittance with respect to different input intensities had been recorded. Then, by fitting the relation between the optical transmission and the input laser power by using the following formula: $T(I) = 1 - \Delta T * \exp(-I/I_{sat}) - T_{ns}$ where, $T(I)$ is the transmission rate, ΔT is the modulation depth, I is the input intensity, I_{sat} is the saturating intensity, and T_{ns} is the non-saturable absorbance, the corresponding nonlinear optical parameters could be characterized. Figure 4.1(b) shows the measured nonlinear transmission curve.

From the analyzed data, the Y₂O₃ film SA has saturable absorption of 38%, saturation intensity of 50.76 MW/cm² and non-saturable loss of 52%, respectively. In comparison with certain 2D materials (B. Chen et al., 2015); MoS₂ (2.15%), MoSe₂ (6.73%), WS₂ (2.53%) and WSe₂ (3.02%), the obtained modulation depth of Y₂O₃ film SA is significantly higher. The saturation intensity is also relatively high due to high resistance of the Y₂O₃ film to photo-bleaching.

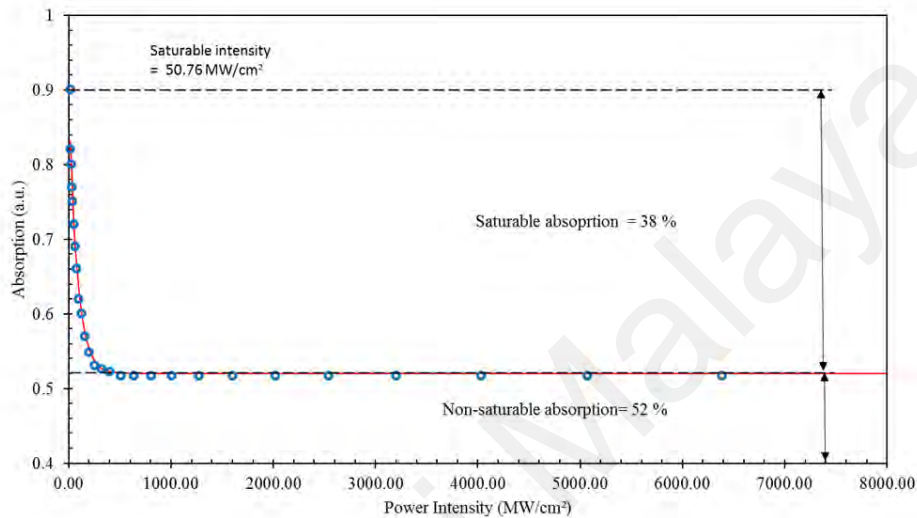
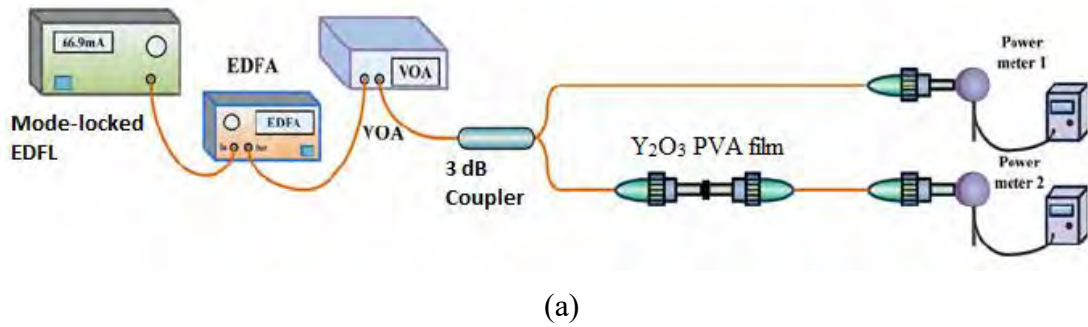


Figure 4.1: (a) The balanced twin-detector measurement system for measuring nonlinear absorption of Y_2O_3 film. (b) The measured saturable absorption characteristic of the film

4.3 Mode-locked laser cavity configuration

The mode-locked EDFL experimental configuration is illustrated in Figure 4.2. The gain medium (2.4 m EDF, IsoGain I-25(980/125)) has peak core absorption of 40 dB/m at 1531 nm wavelength. In addition to that, it also has a core diameter of 4 μm , a cladding diameter of 125 μm and numerical aperture (NA) of 0.23. As shown, the gain medium is optically pumped by a single wavelength 980 nm laser diode (LD) through a 980/1550 nm wavelength division multiplexer (WDM). The light is then channeled into an isolator and the Y_2O_3 film SA. The isolator preserves unidirectional light propagation

within the cavity, whereas the film SA promotes the necessary loss modulation. The integration of the Y_2O_3 film SA into the cavity is done by sandwiching the pre-cut film SA (1 mm x 1 mm) between two FC/PC fibre ferrules. The joining was then closely fitted with a clean fibre adapter. A small quantity of index matching gel was pre-applied onto the surface of the fibre ferrule where the film SA to be located. The application of the gel would minimize the unwanted parasitic reflections. After transmitting out from the SA, the light is then propagated through 200 m single mode fibre (SMF28) before it is directed into a 90/10 optical coupler. 10% of the laser output is channeled out as an output while the remaining 90% is directed into the WDM through the 1550 nm port for a complete closed-loop light propagation. The additional length of SMF28 is used to assist the Y_2O_3 film SA for a stable self-starting mode-locked laser generation by providing sufficient dispersion and nonlinearity in the cavity. As in the mode-locked operation, both of these two parameters; dispersion and nonlinearity need to be well balanced. Furthermore, it would also enhance the pulse energy by slightly broadening the pulse width. This enhanced pulse energy would be sufficient enough to saturate the Y_2O_3 film SA at a moderate pump power.

The EDFL cavity was observed to operate in the anomalous dispersion regime with a group velocity dispersion (GVD) of $\sim 21.9 \text{ ps}^2/\text{km}$. The total net dispersion was calculated to be approximately $\sim -4.464 \text{ ps}^2/\text{km}$. An optical spectrum analyzer (OSA) with a 0.07 nm resolution was utilized to investigate the laser optical spectrum. Meanwhile, a radio frequency spectrum analyzer (RFSA) and a digital oscilloscope (OSC) that pre-coupled with a fast photodetector (PD) was used to examine the presence and quality of the pulsed signal in the time domain and frequency domain, respectively. An optical power meter was also used to measure the laser output power.

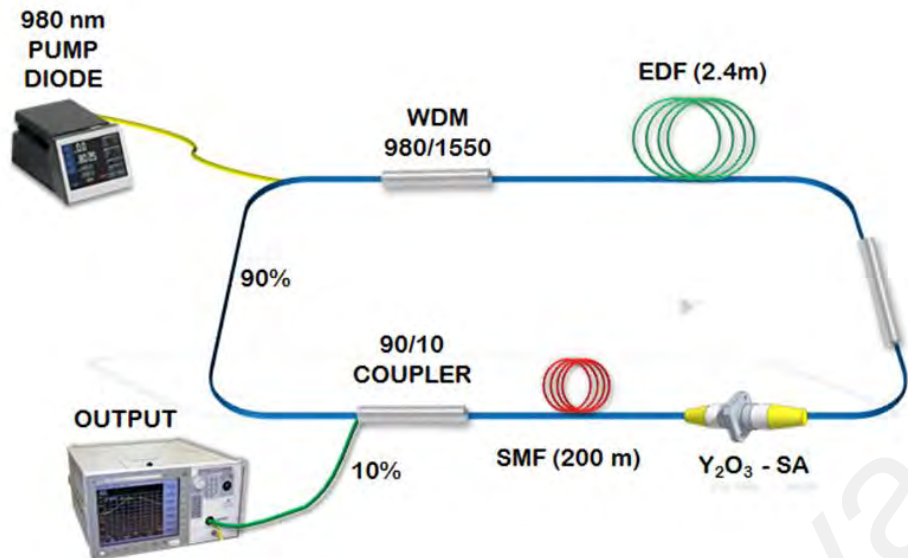


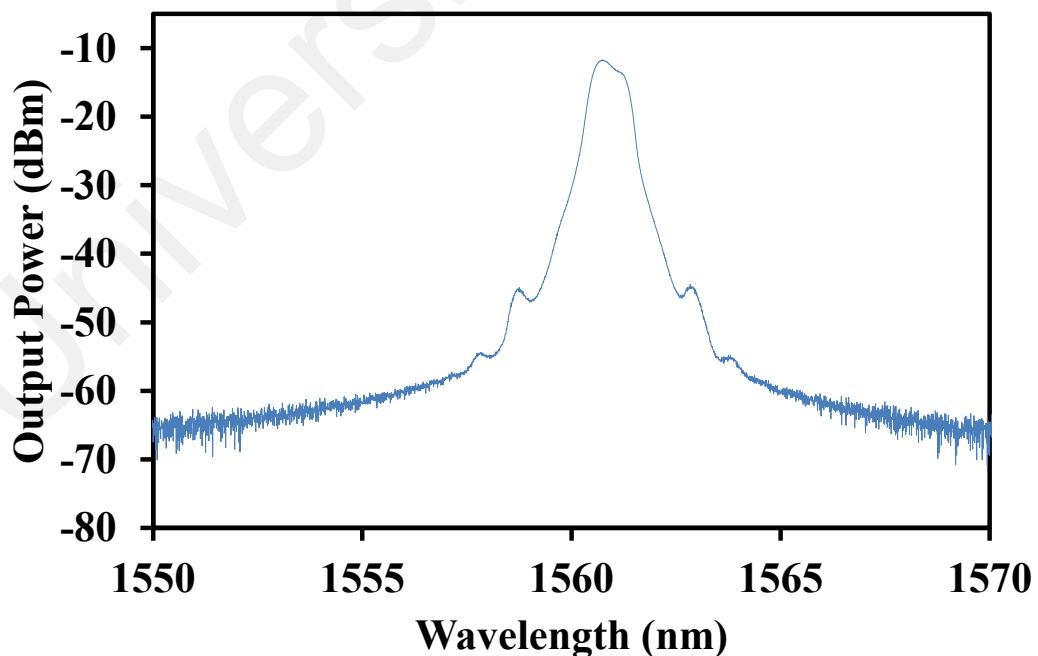
Figure 4.2: Configuration of Y₂O₃ film-based mode-locked EDFL.

4.4 Result and Discussion

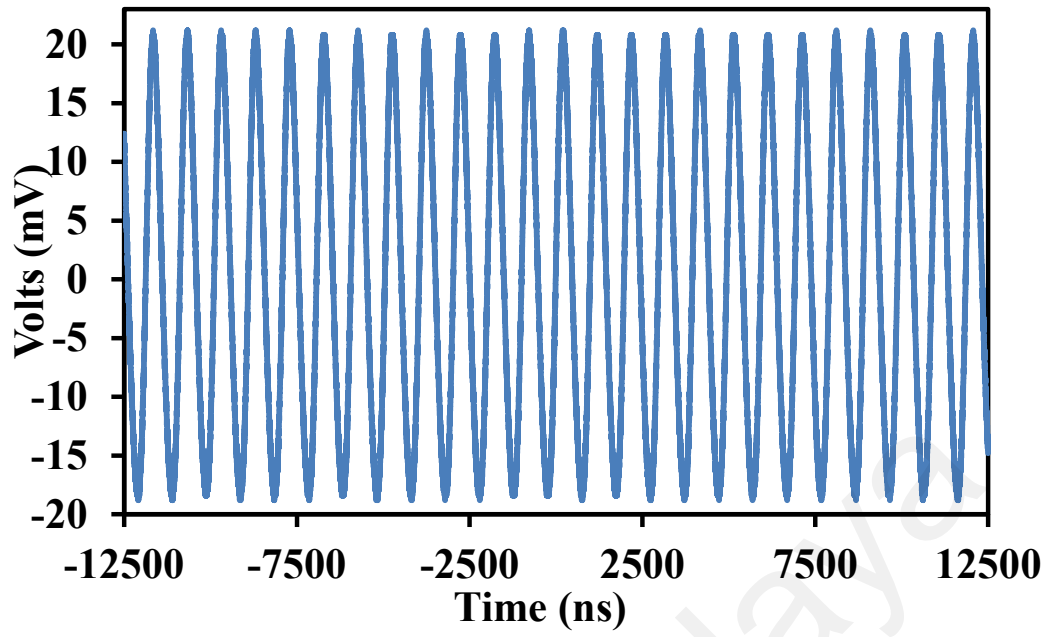
A stable self-starting mode-locking operation was observed, emerging at a threshold pump power of 181.5 mW. The mode-locked laser remained stable as the pump power rose to 246.0 mW. In the mode-locking process, Y₂O₃ SA is utilized to obtain self-amplitude modulation (SAM) in the cavity. The film SA creates some loss inside the cavity, which is relatively large for low intensity, however, fairly small for a short pulse with high intensity. Hence, a short pulse creates a loss modulation due to high intensity at the pulse's peak saturates the absorber strongly than its low intensity wing (Ursula Keller, 2003).

Figure 4.3 shows the mode-locked EDFL important characteristics examined at the threshold pump power of 181.5 mW. Figure 4.3 (a), illustrates the optical spectrum of the mode-locked EDFL. The laser has a central wavelength of 1560.9 nm and a peak power intensity of -11.9 dBm. The 3dB spectral bandwidth is approximately 0.8 nm. Two weak Kelly sidebands were also observed which indicates the mode-locking pulses operate in a soliton regime. The mode-locked pulses train as depicted in Figure 4.3 (b), has a nearly constant repetition rate of 1.0 MHz and has a considerably small amplitude fluctuation (below than 5%).

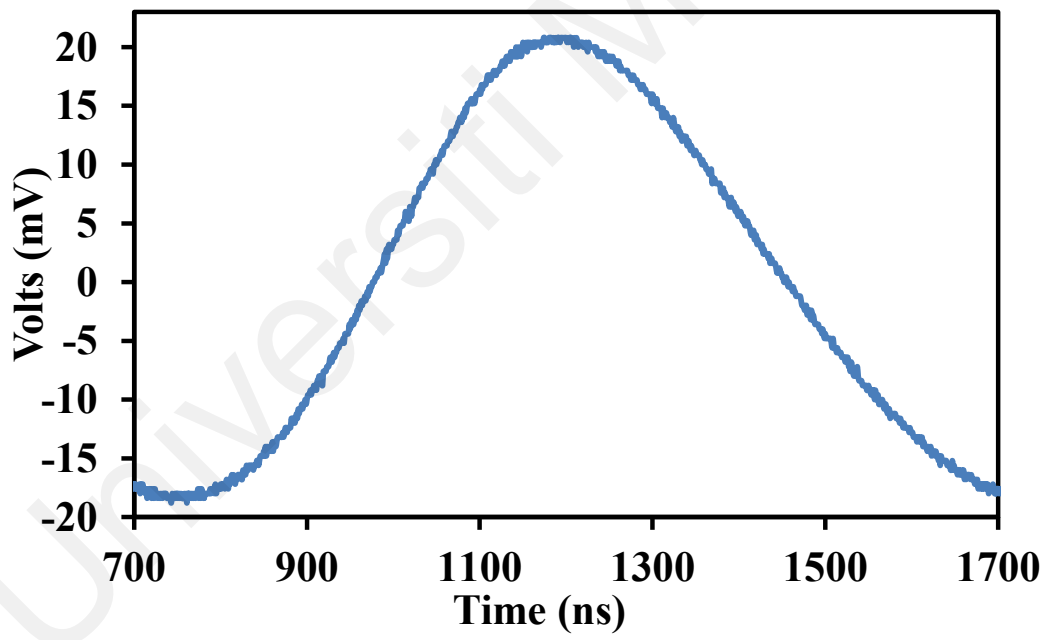
The obtained repetition rate was examined, to be related with the overall EDFL cavity length of 207 m, indicating that the pulsed laser was a mode-locked laser. Figure 4.3 (c) shows the envelope of a single pulse. The pulse width was measured to be approximately 460 ns at full wave half maximum (FWHM). Based on the RF spectrum obtained at 181.5 mW pump power as provided in Figure 4.3(d), the stability of the pulsed laser was further investigated. The fundamental frequency is found to be 1 MHz with 4 harmonics. This result is highly in agreement with the pulse period obtained via the oscilloscope trace. The harmonic trend indicates that the mode-locking pulses are operating in nanosecond regime. From the RF spectrum, it can also be seen that the SNR is high at 57 dB which affirms the stability of the mode-locked pulses. To substantiate that the laser's mode-locking pulse generation was due to the Y_2O_3 , the Y_2O_3 PVA film was replaced with a pristine PVA film. Using this configuration, no pulses was visible on the oscilloscope at any pump power. This affirms that the prepared Sm_2O_3 SA is responsible for the mode-locking operation.



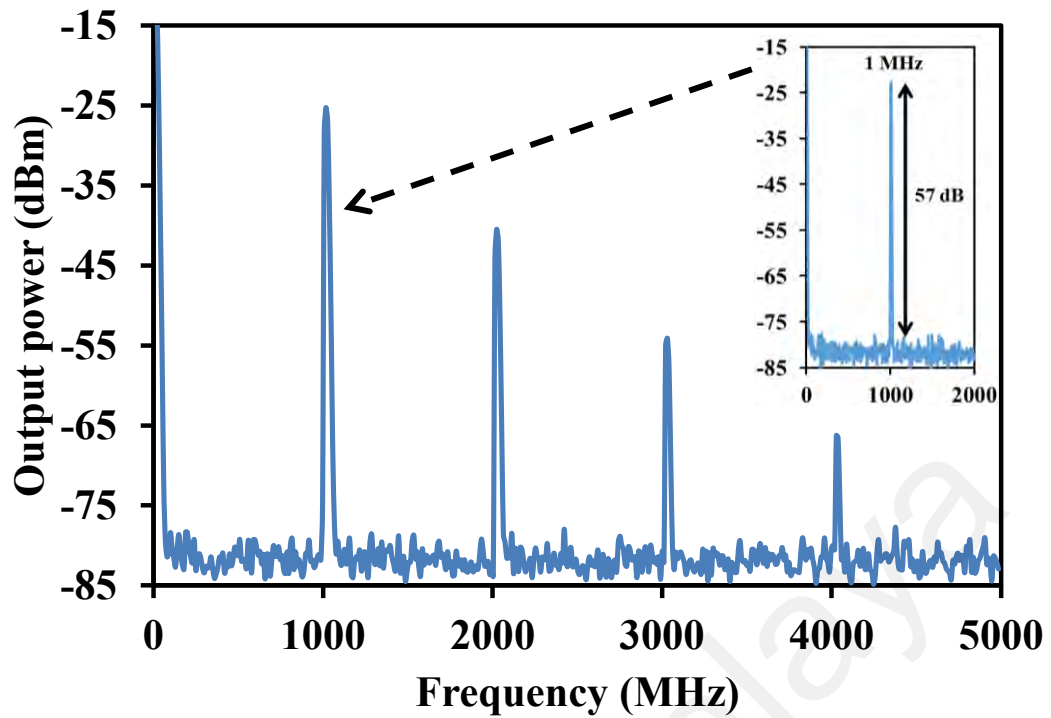
(a)



(b)



(c)



(d)

Figure 4.3: Important characteristics of the Y_2O_3 based mode-locked EDFL at 181.5 mW pump power (a) Output spectrum (b) Oscilloscope trace (c) A single pulse envelop (d) RF spectrum, while the inset shows the fundamental frequency in detail.

Figure 4.4 shows the mode-locked EDFL performances. The output power increases almost linearly from 20.83 mW to the maximum of 25.48 mW, as the pump power increased from 181.5 mW to 246.0 mW. The corresponding slope efficiency is obtained as 7.23 %. The increase of the pump power causes the pulse energy to rise accordingly, to reach the maximum value of 25.2 nJ. The mode-locked operation was examined for 1 hr duration at room temperature. Observation of the laser output showed no significant fluctuations in the optical spectrum and pulse amplitude, thus validating the long stability of the designed system. This also suggests that the SA was still in good condition, indicating that the SA has higher thermal damage threshold than the laser output.

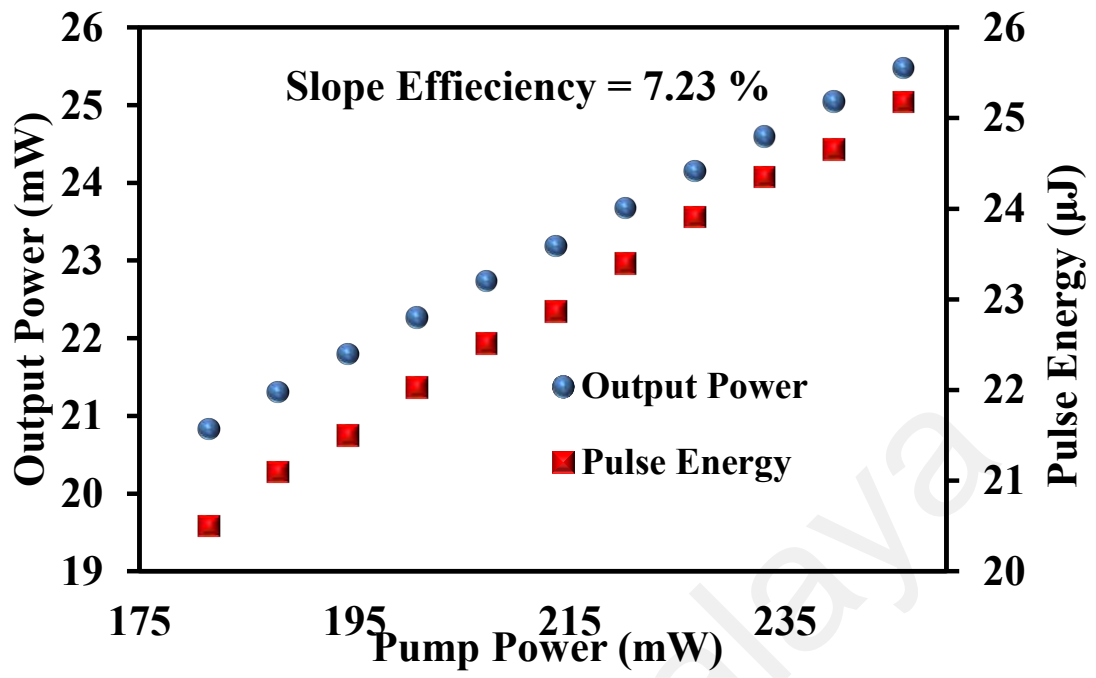


Figure 4.4: The output power and pulse energy of the mode-locked EDFL as a function of pump power (181.5-246.0 mW).

CHAPTER 5: CONCLUSION

The research work aimed to demonstrate both Q-switched and mode-locked Erbium-doped Fiber Lasers (EDFLs) utilizing Yttrium Oxide (Y_2O_3) based saturable absorber (SA). The film SA was prepared through solution casting technique by embedding the Y_2O_3 powder into a polyvinyl alcohol (PVA) host film. A small piece of the fabricated Y_2O_3 film was sandwiched between two ferrules and incorporated into an EDFL cavity, which was optimized for both Q-switching and mode-locking pulse generation experiments.

In this work, the application of Y_2O_3 thin film as a SA was successfully demonstrated for the first time in generating a stable and compact Q-switched EDFL operating at 1560.5 nm. By integrating the fabricated Y_2O_3 film in a laser cavity, a stable pulsed laser appeared when the input pump power hit the threshold at 52.4 mW. The frequency of the pulsed laser rose from 70.22 kHz to 99.2 kHz, matching the increase of pump power from 52.4 mW to 181.5 mW. The shortest pulse width of 2.97 μ s and the maximum pulses energy of 180 nJ were obtained at the pump power of 181.5 mW. In addition, the signal to noise ratio (SNR) of RF signal was obtained at 58 dB, which indicates the excellent stability for the Q-switching pulses.

In another experiment, a passively stable and compact mode-locked EDFL was also realized by integrating Y_2O_3 PVA composite thin film in the ring cavity. By incorporating the film SA along with 200 m long single mode fibre (SMF) into an EDFL cavity, the mode-locked laser with 1 MHz repetition rate stably emerged at an increasing pump power, ranging within 181.5 – 246.0 mW. The pulse width was measured to be 460 ns. The mode-locked laser had a slope efficiency of 7.23 %, while the highest average output power and pulse energy were obtained at 25.48 mW and 25.2 nJ, respectively. The fundamental frequency was examined to have a signal to noise

ratio (SNR) of 57 dB, which suggests that the Y_2O_3 film SA can produce a stable mode-locking pulses.

Based on these results, we can conclude that Y_2O_3 film possess the potential advantage for stable Q-switched and mode-locked pulse generation at 1.5 μm region. There are several aspects that need to be considered for further improvements. First, the cavity length can be further optimized to obtain a better repetition rate and pulse width. Future studies should be focusing on exploring more on the optical property of the SA especially for ultrafast laser generation.

Universiti Malaysia

REFERENCES

- Ab Rahman, M. F., Latiff, A. A., Rosol, A. H. A., Dimiyati, K., Wang, P., & Harun, S. W. (2018). Ultrashort Pulse Soliton Fiber Laser Generation With Integration of Antimony Film Saturable Absorber. *Journal of Lightwave Technology*, 36(16), 3522-3527.
- Adnan, N., Bidin, N., Taib, N., Haris, H., Fakaruddin, M., Hashim, A., . . . Harun, S. (2016a). Passively Q-switched flashlamp pumped Nd: YAG laser using liquid graphene oxide as saturable absorber. *Optics & Laser Technology*, 80, 28-32.
- Adnan, N., Bidin, N., Taib, N., Haris, H., Fakaruddin, M., Hashim, A., . . . Harun, S. W. (2016b). Passively Q-switched flashlamp pumped Nd: YAG laser using liquid graphene oxide as saturable absorber. *Optics & Laser Technology*, 80, 28-32.
- Ahmad, F., Harun, S. W., Nor, R. M., Zulkepely, N., Muhammad, F., Arof, H., & Ahmad, H. (2014). Mode-locked soliton erbium-doped fiber laser using a single-walled carbon nanotubes embedded in polyethylene oxide thin film saturable absorber. *Journal of Modern Optics*, 61(6), 541-545.
- Ahmad, F., Harun, S. W., Nor, R. M., Zulkepely, N. R., Muhammad, F. D., Arof, H., & Ahmad, H. (2014). Mode-locked soliton erbium-doped fiber laser using a single-walled carbon nanotubes embedded in polyethylene oxide thin film saturable absorber. *Journal of Modern Optics*, 61(6), 541-545. doi: 10.1080/09500340.2014.899644
- Anyi, C., Haris, H., Harun, S. W., Ali, N. M., & Arof, H. (2013). Nanosecond pulse fibre laser based on nonlinear polarisation rotation effect. *Electronics Letters*, 49(19), 1240-1241.
- Bao, Q., Zhang, H., Ni, Z., Wang, Y., Polavarapu, L., Shen, Z., . . . Loh, K. P. (2011). Monolayer graphene as a saturable absorber in a mode-locked laser. *Nano Research*, 4(3), 297-307.
- Chen, B., Zhang, X., Wu, K., Wang, H., Wang, J., & Chen, J. (2015). Q-switched fiber laser based on transition metal dichalcogenides MoS₂, MoSe₂, WS₂, and WSe₂. *Optics express*, 23(20), 26723-26737.
- Chen, Y., Jiang, G., Chen, S., Guo, Z., Yu, X., Zhao, C., . . . Tang, D. (2015). Mechanically exfoliated black phosphorus as a new saturable absorber for both Q-switching and Mode-locking laser operation. *Optics Express*, 23(10), 12823-12833.
- Faubert, D., & Chin, S. (1982). Short laser pulse generation: part one. *Optics & Laser Technology*, 14(4), 197-206.
- Fermann, M., Galvanauskas, A., Sucha, G., & Harter, D. (1997). Fiber-lasers for ultrafast optics. *Applied Physics B: Lasers and Optics*, 65(2), 259-275.
- Fermann, M. E., & Hartl, I. (2013). Ultrafast fibre lasers. *Nature photonics*, 7(11), 868.

- Ferrari, A. C., Meyer, J. C., Scardaci, V., Casiraghi, C., Lazzeri, M., Mauri, F., . . . Geim, A. K. (2006). Raman spectrum of graphene and graphene layers. *Phys Rev Lett*, *97*(18), 187401. doi: 10.1103/PhysRevLett.97.187401
- Foster, M. A., Turner, A. C., Sharping, J. E., Schmidt, B. S., Lipson, M., & Gaeta, A. L. (2006). Broad-band optical parametric gain on a silicon photonic chip. *Nature*, *441*(7096), 960.
- Guo, Y. Q., Sun, X. Y., Liu, Y., Wang, W., Qiu, H. X., & Gao, J. P. (2012). One pot preparation of reduced graphene oxide (RGO) or Au (Ag) nanoparticle-RGO hybrids using chitosan as a reducing and stabilizing agent and their use in methanol electrooxidation. *Carbon*, *50*(7), 2513-2523. doi: 10.1016/j.carbon.2012.01.074
- Gupta, M. C., & Ballato, J. (2006). *The handbook of photonics*: CRC press.
- Hakulinen, T., & Okhotnikov, O. G. (2007). 8 ns fiber laser Q switched by the resonant saturable absorber mirror. *Optics Letters*, *32*(18), 2677-2679.
- Haris, H., Harun, S., Anyi, C., Muhammad, A., Ahmad, F., Tan, S., . . . Arof, H. (2015). Generation of soliton and bound soliton pulses in mode-locked erbium-doped fiber laser using graphene film as saturable absorber. *Journal of Modern Optics*, 1-6.
- Haus, H. A. (2000). Mode-locking of lasers. *IEEE Journal of Selected Topics in Quantum Electronics*, *6*(6), 1173-1185.
- Island, J. O., Steele, G. A., van der Zant, H. S., & Castellanos-Gomez, A. (2015). Environmental instability of few-layer black phosphorus. *2D Materials*, *2*(1), 011002.
- Ismail, M. A., Harun, S. W., Zulkepely, N. R., Nor, R. M., Ahmad, F., & Ahmad, H. (2012). Nanosecond soliton pulse generation by mode-locked erbium-doped fiber laser using single-walled carbon-nanotube-based saturable absorber. *Applied Optics*, *51*(36), 8621-8624. doi: 10.1364/Ao.51.008621
- Kang, Z., Liu, M., Li, Z., Li, S., Jia, Z., Liu, C., . . . Qin, G. (2018). Passively Q-switched erbium doped fiber laser using a gold nanostars based saturable absorber. *Photonics Research*, *6*(6), 549-553.
- Keller, U. (2003). Recent developments in compact ultrafast lasers. *nature*, *424*(6950), 831.
- Keller, U. (2003). Recent developments in compact ultrafast lasers. *Nature*, *424*(6950), 831-838. doi: 10.1038/nature01938
- Keller, U., Miller, D., Boyd, G., Chiu, T., Ferguson, J., & Asom, M. (1992). Solid-state low-loss intracavity saturable absorber for Nd: YLF lasers: an antiresonant semiconductor Fabry–Perot saturable absorber. *Optics letters*, *17*(7), 505-507.

- Laroche, M., Chardon, A. M., Nilsson, J., Shepherd, D. P., Clarkson, W. A., Girard, S., & Moncorge, R. (2002). Compact diode-pumped passively Q-switched tunable Er-Yb double-clad fiber laser. *Opt Lett*, 27(22), 1980-1982.
- Li, H., Xia, H., Lan, C., Li, C., Zhang, X., Li, J., & Liu, Y. (2015). Passively Q-switched erbium-doped fiber laser based on few-layer MoS₂ saturable absorber. *IEEE Photonics Technology Letters*, 27(1), 69-72.
- Lin, Y.-H., Yang, C.-Y., Liou, J.-H., Yu, C.-P., & Lin, G.-R. (2013). Using graphene nano-particle embedded in photonic crystal fiber for evanescent wave mode-locking of fiber laser. *Optics express*, 21(14), 16763-16776.
- Liu, J., Xu, J., & Wang, P. (2012). Graphene-based passively Q-switched 2 μ m thulium-doped fiber laser. *Optics Communications*, 285(24), 5319-5322.
- Liu, S., Yan, J., He, G., Zhong, D., Chen, J., Shi, L., . . . Jiang, H. (2012). Layer-by-layer assembled multilayer films of reduced graphene oxide/gold nanoparticles for the electrochemical detection of dopamine. *Journal of Electroanalytical Chemistry*, 672, 40-44.
- Lucas, L., & Zhang, J. (2012). Femtosecond laser micromachining: a back-to-basics primer. *Industrial laser solutions*.
- Luo, Z.-C., Liu, J.-R., Wang, H.-Y., Luo, A.-P., & Xu, W.-C. (2012). Wide-band tunable passively Q-switched all-fiber ring laser based on nonlinear polarization rotation technique. *Laser physics*, 22(1), 203-206.
- Luo, Z., Zhou, M., Weng, J., Huang, G., Xu, H., Ye, C., & Cai, Z. (2010). Graphene-based passively Q-switched dual-wavelength erbium-doped fiber laser. *Optics letters*, 35(21), 3709-3711.
- Markom, A., Tan, S., Haris, H., Paul, M., Dhar, A., Das, S., & Harun, S. (2018). Experimental Observation of Bright and Dark Solitons Mode-Locked with Zirconia-Based Erbium-Doped Fiber Laser. *Chinese Physics Letters*, 35(2), 024203.
- Matniyaz, T. (2018). Free-space NPR mode locked erbium doped fiber laser based frequency comb for optical frequency measurement. *arXiv preprint arXiv:1802.10183*.
- Meiser, N. (2013). *Novel Technologies for Mode-Locking of Solid-State Lasers*. KTH Royal Institute of Technology.
- Niu, K., Chen, Q., Sun, R., Man, B., & Zhang, H. (2017). Passively Q-switched erbium-doped fiber laser based on SnS₂ saturable absorber. *Optical materials express*, 7(11), 3934-3943.
- Noda, H., Muramoto, K., & Kim, H. (2003). Preparation of nano-structured ceramics using nanosized Al₂O₃ particles. *Journal of materials science*, 38(9), 2043-2047.

- Paschotta, R., Häring, R., Gini, E., Melchior, H., Keller, U., Offerhaus, H., & Richardson, D. (1999). Passively Q-switched 0.1-mJ fiber laser system at 1.53 μm. *Optics letters*, 24(6), 388-390.
- Paschotta, R., & Keller, U. (2003). Ultrafast solid-state lasers. *Ultrafast Lasers: Technology and Applications*, 1-60.
- Philippov, V. N., Kir'yanov, A. V., & Unger, S. (2004). Advanced Configuration of Erbium Fiber Passively Q-Switched Laser With Co²⁺:ZnSe Crystal as Saturable Absorber. *IEEE Photonics Technology Letters*, 16(1), 57-59. doi: 10.1109/lpt.2003.819397
- Popa, D., Sun, Z., Hasan, T., Torrisi, F., Wang, F., & Ferrari, A. C. (2011). Graphene Q-switched, tunable fiber laser. *Applied Physics Letters*, 98(7), 073106.
- Popa, D., Sun, Z., Hasan, T., Torrisi, F., Wang, F., & Ferrari, A. C. (2011). Graphene Q-switched, tunable fiber laser. *Applied Physics Letters*, 98(7). doi: Artn 073106
10.1063/1.3552684
- Popa, D., Sun, Z., Torrisi, F., Hasan, T., Wang, F., & Ferrari, A. C. (2010). Sub 200 fs pulse generation from a graphene mode-locked fiber laser. *Applied Physics Letters*, 97(20). doi: Artn 203106
10.1063/1.3517251
- Rahman, M., Rusdi, M., Lokman, M., Mahyuddin, M., Latiff, A., Rosol, A., . . . Harun, S. (2017). Holmium Oxide Film as a Saturable Absorber for 2 μm Q-Switched Fiber Laser. *Chinese Physics Letters*, 34(5), 054201.
- Riesbeck, T., & Lux, O. (2009). AOM fourfold pass for efficient Q-switching and stable high peak power laser pulses. *Optics Communications*, 282(18), 3789-3792. doi: 10.1016/j.optcom.2009.06.039
- Rozhin, A. G., Sakakibara, Y., Tokumoto, M., Kataura, H., & Achiba, Y. (2004). Near-infrared nonlinear optical properties of single-wall carbon nanotubes embedded in polymer film. *Thin Solid Films*, 464, 368-372. doi: 10.1016/j.tsf.2004.07.005
- Saleh, Z., Anyi, C., Haris, H., Ahmad, F., Ali, N., Harun, S., & Arof, H. (2014). Q-switched Erbium-doped fiber laser using multi-layer graphene oxide based saturable absorber. *OPTOELECTRONICS AND ADVANCED MATERIALS-RAPID COMMUNICATIONS*, 8(7-8), 626-630.
- Set, S. Y., Yaguchi, H., Tanaka, Y., & Jablonski, M. (2004). Laser mode locking using a saturable absorber incorporating carbon nanotubes. *Journal of Lightwave Technology*, 22(1), 51.
- Siegman. (1986).
- Skorczakowski, M., Swiderski, J., Pichola, W., Nyga, P., Zajac, A., Maciejewska, M., . . . Heinrich, A. (2010). Mid-infrared Q-switched Er: YAG laser for medical applications. *Laser Physics Letters*, 7(7), 498.

- Spuhler, G. J., Weingarten, K. J., Grange, R., Krainer, L., Haiml, M., Liverini, V., . . . Keller, U. (2005). Semiconductor saturable absorber mirror structures with low saturation fluence. *Applied Physics B-Lasers and Optics*, 81(1), 27-32. doi: 10.1007/s00340-005-1879-1
- Svelto, O., & Hanna, D. C. (1998). *Principles of lasers* (Vol. 4): Springer.
- Trebino, R. (2012). *Frequency-resolved optical gating: the measurement of ultrashort laser pulses*: Springer Science & Business Media.
- Vasseur, J. (2006). *Multiwavelength laser sources for broadband optical access networks*. Georgia Institute of Technology.
- Wang, M., Chen, C., Huang, C., & Chen, H. (2014). Passively Q-switched Er-doped fiber laser using a semiconductor saturable absorber mirror. *Optik-International Journal for Light and Electron Optics*, 125(9), 2154-2156.
- Wang, W., Meng, H., Wu, X., Xiong, R., Xue, H., Tan, C., & Huang, X. (2012). A nonlinear polarization rotation-based linear cavity waveband switchable multi-wavelength fiber laser. *Laser Physics Letters*, 10(1), 015104.
- Xinju, L. (2010). *Laser technology*: CRC press.
- Yang, H., Withers, F., Gebremedhn, E., Lewis, E., Britnell, L., Felten, A., . . . Casiraghi, C. (2014). Dielectric nanosheets made by liquid-phase exfoliation in water and their use in graphene-based electronics. *2D Materials*, 1(1), 011012.
- Yin, Z., He, Q., Huang, X., Zhang, J., Wu, S., Chen, P., . . . Zhang, H. (2012). Real-time DNA detection using Pt nanoparticle-decorated reduced graphene oxide field-effect transistors. *Nanoscale*, 4(1), 293-297.
- Zhao, Y., Chen, Z., Saxer, C., Xiang, S., de Boer, J. F., & Nelson, J. S. (2000). Phase-resolved optical coherence tomography and optical Doppler tomography for imaging blood flow in human skin with fast scanning speed and high velocity sensitivity. *Optics Letters*, 25(2), 114-116.
- Zhou, D.-P., Wei, L., Dong, B., & Liu, W.-K. (2010). Tunable passively Q-switched erbium-doped fiber laser with carbon nanotubes as a saturable absorber. *IEEE Photonics Technology Letters*, 22(1), 9-11.